Acetophenone Derivatives from a Freshwater Fungal Isolate of Recently Described Lindgomyces Madisonensis (G416)

By: Noemi D. Paguigan, Huzefa A. Raja, Cynthia S. Day, and Nicholas H. Oberlies

"Acetophenone Derivatives from a Freshwater Fungal Isolate of Recently Described Lindgomyces Madisonensis (G416)." Noemi D. Paguigan, Huzefa A. Raja, Cynthia S. Day, and Nicholas H. Oberlies. *Phytochemistry, 2016*, *126,* 59-65. PMID: 26988728; doi: 10.1016/j.phytochem.2016.03.007

Abstract:

The exploration of freshwater ascomycetes, which have undergone only limited investigation, may provide opportunities both to characterize new genera/species of fungi and to uncover new chemical diversity. In this study, seven acetophenone derivatives, madisone, 4′-methoxymadisone, dehydromadisone, 2″-methoxymadisone, dihydroallovisnaginone, dimadisone, and 4′-methoxydimadisone were characterized from an organic extract of a recently described *Lindgomyces madisonensis* (G416) culture, which was isolated from submerged wood collected in a stream in North Carolina. Madisone, dehydromadisone, 2″-methoxymadisone, dimadisone and 4′-demethoxydimadisone have not been reported previously, while 4′-methoxymadisone and dihydroallovisnaginone were previously unknown as natural products. Their structures were assigned on the basis of NMR and HRESIMS data, with the structure of madisone supported by X-ray crystallography. The antimicrobial activities of madisone, 4′-methoxymadisone and dihydroallovisnaginone were evaluated against a panel of bacteria and fungi. A heat map analysis of the surface of a G416 culture showed that most of the isolated compounds concentrated in the guttate compared with the vegetative mycelium of the fungus.

Keywords: Submerged wood | *Lindgomyces madisonensis* | Freshwater ascomycetes | Acetophenones

Article:

Abbreviations: $CHCl_3$, chloroform; CH_3OH, methanol; CH_3CN, acetonitrile; NMR, nuclear magnetic resonance; HRESIMS, high-resolution electrospray ionization mass spectrometry; HPLC, high-performance liquid chromatography; HMBC, heteronuclear multiple bond coherence; HSQC, heteronuclear single quantum coherence; CD_3OD, deuterated methanol; $CDCl_3$, deuterated chloroform; ITS rDNA, internal transcribed spacer region of ribosomal deoxyribonucleic acid; DNA, deoxyribonucleic acid; PCR, polymerase chain reaction; BLAST, basic

1. Introduction

Fungi represent a highly diverse group of organisms, and even though there exists an estimated 5.1 million species, less than 100 thousand have been cultivated and described (Blackwell, 2011), and only a fraction of those have been studied with respect to their chemistry (Aly et al., 2011). Freshwater ascomycetes are an ecological group that occur on submerged substrates in fresh water and play an important role as decomposers in these habitats (Shearer, 1993, Shearer, 2007, Shearer and Raja, 2015). The number of described ascomycetes has increased dramatically over the past 25 years. Shearer (1993) reported about 200 species from freshwater habitats worldwide; that number doubled to 414 in a 2001 review (Shearer, 2001). Currently, about 640 freshwater ascomycetes have been described (Shearer and Raja, 2015). While knowledge regarding the distribution patterns and taxonomy has increased for this ecological group of fungi due to intensive collection over the last two decades, their chemistry, particularly regarding secondary metabolites, has had limited investigation (Hosoe et al., 2010, Jiao et al., 2006, Li et al., 2003, Mudur et al., 2006, Oh et al., 1999, Reategui et al., 2005). As of 2011, approximately 127 chemical structures had been reported from about 30–40 freshwater fungal species (El-Elimat et al., 2014a, El-Elimat et al., 2014b, Hernández-Carlos and Gamboa-Angulo, 2011). To ameliorate this knowledge gap, studies were initiated on the chemical mycology of freshwater ascomycetes in North Carolina, USA (El-Elimat et al., 2014a, El-Elimat et al., 2014b, Raja et al., 2015, Raja et al., 2013a, Raja et al., 2013b), representing the first systematic study of freshwater ascomycetes from this region of North America. Ongoing investigations led to the isolation of five new acetophenones (**1**, **3**, **4**, **6**, and **7**), along with 4′-methoxymadisone (**2**) and dihydroallovisnaginone (**5**), from a fungal isolate recently described as *Lindgomyces madisonensis* (G416) Raja & Oberlies (Crous et al., 2015). A heat map analysis by *in situ* sampling via droplet-liquid microjunction-surface sampling probe (droplet-LMJ-SSP) of a *L. madisonensis* (G416) culture showed that the isolated compounds were more abundant in the guttate compared to the fungal mycelium.

2. Results and discussion

2.1. Structural characterization and bioactivity of compounds **1**–**7**

A culture of *L. madisonensis* (G416) was isolated from decomposing wood collected in the central Piedmont region of North Carolina. The fungus was cultured by solid-substrate fermentation on rice, and this material was extracted with 1:1 $CHCl_3$–CH_3OH. The resulting extract was subjected to partitioning with organic solvents followed by purification using flash chromatography yielding five fractions. These fractions were further purified using preparative HPLC, leading to the isolation of compounds **1**–**7** (Fig. 1). The structures of these were established by analysis of spectroscopic (NMR) and spectrometric (HRESIMS) data.

---

local alignment search tool; PDA, potato dextrose agar; YESD, yeast extract soy dextrose; ELSD, evaporative light scattering detector; UV, ultraviolet; amu, atomic mass unit; Droplet-LMJ-SSP, droplet-liquid microjunction-surface sampling probe

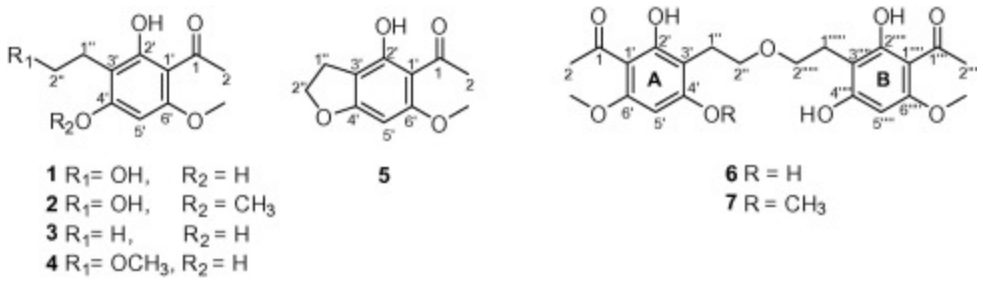

Fig. 1. Structures of compounds **1**–**7**.

On the basis of HRESIMS and NMR data (Table 1 and Fig. S1), compound **1** was found to have the molecular formula $C_{11}H_{14}O_5$ (five degrees of unsaturation). The IR spectrum of **1** showed absorption bands at 2972 and 1610 cm^{-1}, indicative of an aromatic ring with chelated hydroxy and carbonyl moieties; these functionalities were supported by the observed UV absorption maxima at 306 and 237 nm. ^{13}C NMR and HSQC data, indicated 11 carbon signals, which were attributed to six aromatic carbons (five nonprotonated and one protonated), one ketone carbonyl, and four carbon signals located in the aliphatic region of the spectrum. Furthermore, chemical shift data indicated that three of the aromatic carbons were oxygenated (δ_C 163.3, 166.1, 164.7 for C-6′, C-2′, and C-4′, respectively). The downfield region of the ^1H NMR spectrum of **1** exhibited a singlet at δ_H5.98 that integrated for one aromatic proton, as expected for a penta-substituted benzene ring. Based on the ^1H NMR data (Table 1), the structure of **1** had one isolated methyl group (δ_H 2.55, singlet), one methoxy, and a hydroxyethyl group. The connections between the subunits were deduced from key HMBC correlations (Fig. 2), including: H-5′ to C-6′, C-1′, C-3′, and C-4′; the methoxy to C-6′; the isolated methyl H_3-2 to C-1′; and H_2-1″ and H_2-2″ of the hydroxyethyl group to C-2′, C-3′, and C-4′, and to C-3′, respectively. In further efforts to verify the locations of subunits on the aromatic ring, ^1H NMR data for **1** were recorded in $CDCl_3$, revealing a singlet resonance at δ_H 14.58 that was not observed when recorded in CD_3OD (Fig. S8). This result was consistent with the downfield shift associated with intramolecular H-bonding between the proton of the C-2′ hydroxy group and the oxygen of the C-1 carbonyl. The structure of **1**, recrystallized from CH_3OH, was unambiguously assigned by X-ray crystallography (Fig. S23) and ascribed the trivial name, madisone.

Compound **2** was assigned the molecular formula $C_{12}H_{16}O_5$ (five degrees of unsaturation) on the basis of HRESIMS and NMR data. The NMR spectroscopic data for **2** (Table 1) were nearly identical to that of compound **1**, but with additional signals for a second methoxy group (δ_C/δ_H 56.1/3.93), which were consistent with a 14 amu mass difference. A key HMBC correlation was observed from the methoxy group to C-4′, confirming its connectivity and establishing the structure of **2** (Fig. 1, Fig. 2 and S10). Compound **2** was first described as one of the intermediates in an attempted synthetic oxidative approach to LL-D253α (Wootton, 2000). Their data were acquired in $CDCl_3$; the data herein (Fig. S8) were consistent with the literature with one caveat. It is considered that there was an error in the previous assignment of the C-3′ chemical shift value (Wootton, 2000). Thus, we have included the NMR shift assignments of **2**. As this is the first report of the isolation of **2** from a natural source, it was given the trivial name 4′-methoxymadisone.

Table 1. ^{1}H NMR and ^{13}C NMR Spectroscopic Data for compounds **1**–**6** in CD_3OD.

Position	**1**[a]		**2**[a]		**3**[a]		**4**[b]		**5**[a]		**6**[a]	
	δ_C	δ_H, mult (*J* in Hz)	δ_C	δ_H, mult (*J* in Hz)	δ_C	δ_H, mult (*J*in Hz)	δ_C	δ_H, mult (*J*in Hz)	δ_C	δ_H, mult (*J* in Hz)	δ_C	δ_H, mult (*J* in Hz)
1	204.2		204.8		204.2		204.1		204.4		204.2	
2	33.1	2.55, s	33.4	2.58, s	33.1	2.56, s	33.0	2.56, s	33.1	2.55, s	33.1	2.56, s
1′	105.9		106.6		105.9		105.9		106.8		105.9	
2′	166.1		164.9		165.6		166.1		162.7		166.1	
3′	105.6		106.6		111.2		105.4		106.3		105.5	
4′	164.7		165.7		164.0		[#]164.9		169.3		164.7	
5′	91.2	5.98, s	87.4	6.16, s	91.0	5.98, s	91.4	5.99, s	86.7	6.06, s	91.3	5.99, s
6′	163.3		163.9		162.8		163.4		165.8		163.4	
1″	26.7	2.82, t (7.6)	26.6	2.82, t (7.6)	16.3	2.54, q(7.3)	23.4	2.84, t (7.6)	26.6	3.05, t (7.6)	23.6	2.84, t (7.3)
2″	62.0	3.61, t (7.6)	61.8	3.55, t (7.6)	13.8	1.04, t (7.3)	72.6	3.48, t (7.6)	74.4	4.65, t (7.6)	70.6	3.55, t (7.3)
4′-OCH_3	n/a	–	[*]56.2	3.91, s	n/a	–	n/a	–	n/a	–	n/a	–
6′-OCH_3	55.9	3.84, s	[*]56.1	3.93, s	55.8	3.84, s	55.9	3.85, s	56.3	3.86, s	55.7	3.85, s
2″-OCH_3	n/a	–	n/a	–	n/a	–	58.5	3.36, s	n/a	–	n/a	–

n/a, Not applicable.

[a] Data were collected at 400 MHz (^{1}H) or 100 MHz (^{13}C).

[b] Data were collected at 700 MHz (^{1}H) or 175 MHz (^{13}C).

[*] May be interchanged.

[#] Value deduced from HMBC.

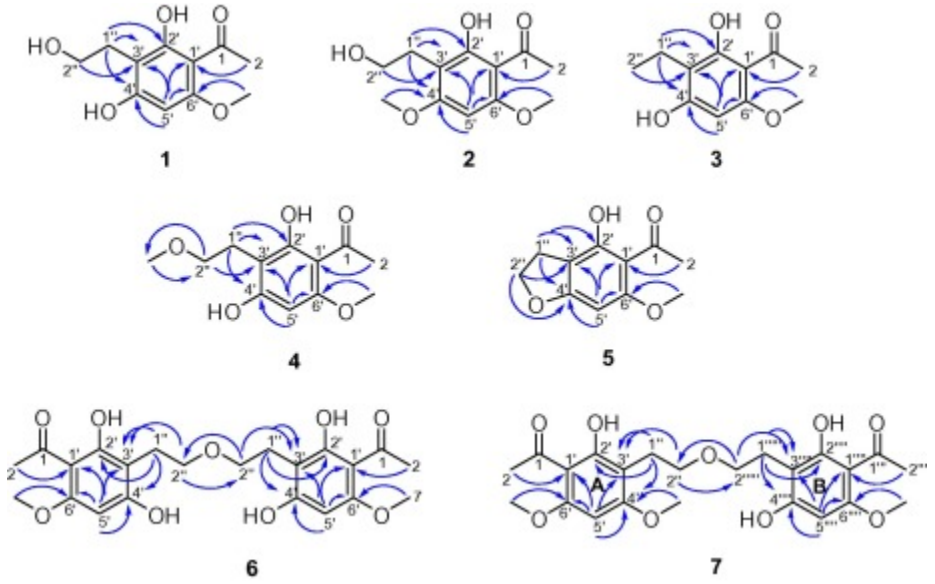

Fig. 2. Key HMBC correlations of compounds **1**–**7**.

The HRESIMS and NMR data established the molecular formula for compound **3** as $C_{11}H_{14}O_4$ (five degrees of unsaturation). Comparison of these data to those of compound **1** indicated the loss of the hydroxy moiety at C-2″, which was consistent with the associated changes in the shifts and the multiplicities of H_2-1″ (δ_H 2.54, quartet, 7.3 Hz) and H_3-2″ (δ_H1.04, triplet, 7.3 Hz); it also accounted for the 16 amu mass difference between these compounds. As such, compound **3** was identified as shown (Fig. 1) and assigned the trivial name dehydromadisone.

The molecular formula of compound **4** was deduced as $C_{12}H_{16}O_5$ (five degrees of unsaturation) based on HRESIMS and NMR data. The NMR and HRMS of **4** suggested structural similarities to **1**. However, **4** had an additional methoxy unit (δ_C/δ_H 58.5/3.36) as evidenced by a 14 amu difference in the HRMS between **1** and **4**. Further analysis of the 1- and 2-D NMR data indicated that the 2″-OH in **1** was replaced with a methoxy unit in **4**. This substitution was confirmed by the observed more downfield C-2″ shift in **4** (δ_C 72.6) compared to the C-2″ shift in **1** (δ_C 62.0). Conversely, C1″ appeared more upfield in **4** compared to **1** at δ_C 23.4 and δ_C 26.7, respectively. Moreover, an HMBC correlation observed for the methoxy protons to C-2″ (Fig. 2 and Fig. S12) established its connectivity. Thus, the structure of compound **4** was assigned (Fig. 1) and ascribed the trivial name 2″-methoxymadisone.

Compound **5** was found to have the molecular formula $C_{11}H_{12}O_4$ (six degrees of unsaturation) on the basis of HRESIMS and NMR data. The ^{1}H NMR spectrum of **5**exhibited signals that were almost identical to those of **1** but with more deshielded H_2-1″ and H_2-2″ resonances at δ_H 3.05 (triplet, 7.6 Hz) and δ_H 4.65 (triplet, 7.6 Hz), respectively. This distinct change in the chemical shift values suggested a heterocycle, which also accounted for the additional unsaturation and the 18 amu mass difference between **1** and **5**(Fig. 1). Although this is the first report of the isolation of **5** from a natural source, Geissman and Hinreiner described it (and named it dihydroallovisnaginone) as one of the derivatives in the monomethylation of 4,6-dihydroxy-5-acetylcoumarane in an attempt to synthesize visnaginone (Geissman and Hinreiner, 1951). Although NMR and HRMS data were not available in 1951, the UV data were consistent with the literature.

The ^{1}H and ^{13}C NMR data of **6** (Table 1) showed signals that were nearly identical to those of **1**. However, the HRMS data established the molecular formula to be $C_{22}H_{26}O_9$ (ten degrees of unsaturation), which indicated twice as many carbons, along with 12 additional hydrogen and four more oxygen atoms relative to the formula of **1**. Compound **6** was presumed to be a homodimer of **1** with an ether linkage connecting the two halves. The HMBC correlation from H_2-2″ (δ_H 3.55) to C-2″ (δ_C 70.6) implied that the two symmetrical units of the compound were connected via the oxygen atom of the hydroxyethyl group comprised of C-1″ and C-2″ (Fig. 2). Therefore, the structure of **6** was proposed as shown in Fig. 1 and ascribed the trivial name dimadisone.

Compound **7** was shown to have the molecular formula $C_{23}H_{28}O_9$ (ten degrees of unsaturation) based on analyses of the HRESIMS and NMR data. The ^{1}H and ^{13}C NMR data (Table 2) displayed two sets of signals, which had close resemblance to those of compounds **1** and **2**, indicating that **7** was a heterodimer of these compounds. In ring A, H-5′ (δ_H 6.17, s) showed HMBC correlations to C-1′ (δ_C 106.7), C-3′ (δ_C 106.6), C-4′ (δ_C165.7), C-6′ (δ_C 164.0); 6′-OCH_3 (δ_H 3.95, s) to C-6′; H-2 (δ_H 2.59, s) to C-1′; and 4′-OCH_3(δ_H 3.93, s) to C-4′. Furthermore, in ring A, H-1″ (δ_H 2.85, m) displayed HMBC correlations to C-2′, C-3′, and C-4′. In ring B, HMBC correlations were observed from H-5‴′ (δ_H 5.98, s) to C-1‴′ (δ_C 106.0), C-3‴′ (δ_C 105.7), C-4‴′ (δ_C 164.9), C-6‴′ (δ_C 163.4); from 6‴′-OCH_3 (δ_H3.85, s) to C-6‴′; and H-2‴′ (δ_H 2.56, s) to C-1‴′ (Fig. 2). Additionally, in ring B, H-1‴′ (δ_H2.82, m) showed HMBC correlations to C-2‴′, C-3‴′, and C-4‴′. The observed key HMBC correlations from H_2-2″ (δ_H 3.54, m) of ring A to C-2‴′ (δ_C 70.5) of ring B, and from H_2-2‴′ (δ_H 3.55, m) of ring B to C-2″ (δ_C 70.3) of ring A, indicated that an ether linkage connected the two halves, similar to that

of **6**. Hence, the structure of **7** was established as shown and was ascribed the trivial name 4′-methoxydimadisone (Fig. 1).

Table 2. ^{1}H NMR and ^{13}C NMR spectroscopic data for compound **7** in CD_3OD.

Position	**7**		
	δ_C	**type**	δ_H, **mult (*J* in Hz)**
Fragment A			
1	204.8	C	
2	33.3	CH_3	2.59, s
1′	106.7	C	
2′	164.9	C	
3′	106.6	C	
4′	165.7	C	
5′	87.5	CH	6.17, s
6′	164.0	C	
1″	23.4	CH_2	2.85, m
2″	**70.3	CH_2	3.54, m
4′-OCH_3	*56.2		3.93, s
6′-OCH_3	*56.1		3.95, s
Fragment B			
1‴	204.2	C	
2‴	33.1	CH_3	2.56, s
1⁗	106.0	C	
2⁗	166.1	C	
3⁗	105.7	C	
4⁗	164.9	C	
5⁗	91.5	CH	5.98, s
6⁗	163.4	C	
1⁗′	23.7	CH_2	2.82, m
2⁗′	**70.5	CH_2	3.55, m
6⁗-OCH_3	55.9		3.85, s

Data were collected at 700 MHz (^{1}H) or 175 MHz (^{13}C).

* May be interchanged.

** May be interchanged.

The structure of **1** was confirmed by X-ray crystallography, and the remaining compounds (**2**–**7**) were structurally related to it via biosynthetic considerations. In particular, the acetophenone moiety was a common motif, noted through the nearly identical NMR data. In addition, when ^{1}H NMR data were acquired in $CDCl_3$, all compounds exhibited a singlet resonance in the range from δ_H 14.00 to δ_H 14.47 (Fig. S8), indicative of chelation between the hydroxy and carbonyl moieties in all of the structures.

Compounds **1**, **2** and **5** were evaluated for antimicrobial activity against *Staphylococcus aureus*, *Escherichia coli*, *Mycobacterium smegmatis*, *Candida albicans*, and *Aspergillus niger* (Table S2). All the compounds tested had minimal inhibitory concentrations greater than 55 μg/mL. Compounds **3**, **4**, **6**, **7** were not evaluated for their antimicrobial activity due to the relative paucity of these samples.

2.2. *In situ* analysis of the concentration of compounds **1**–**7** in *L. madisonensis (G416) cultures*

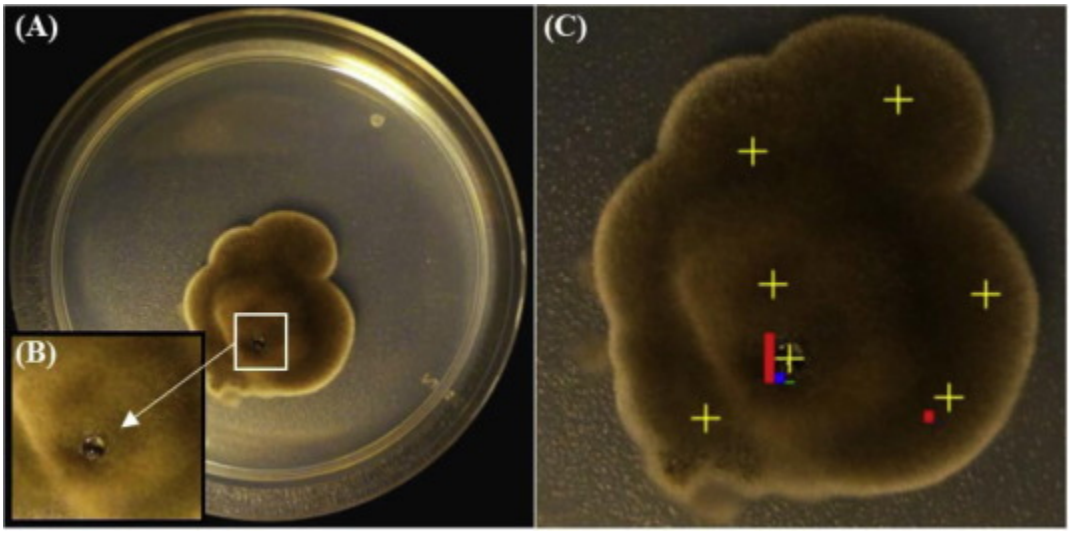

Fig. 3. (A) A three-week-old culture of *L. madisonensis* (G416) grown on PDA producing a guttate. (B) Arrow showing a magnified view of the guttate. (C) Heat map of compounds **1** (red), **2** (and/or) **4** (blue), and **5** (green). The height of the bars indicates the relative amount of signal detected by HRESIMS within a 5 ppm mass tolerance for the given compounds. The crosshairs indicate the sampling points of the droplet-LMJ-SSP.

A 3-week old culture of *L. madisonensis* (G416) growing on PDA at room temperature (~22–25 °C) in a Petri dish sealed with parafilm was noted to produce a clear guttate (exudate) (Fig. 3). An older culture grown under the same conditions did not produce any visible guttates. A few recent studies have suggested that guttates are a rich source of secondary metabolites, although their ecological roles and functions in fungi are still uncertain (Figueroa et al., 2014, Gareis and Gareis, 2007, Wang et al., 2010). It was hypothesized here that guttates may serve to store secondary metabolites, concentrating them for interaction with their environment. To test this, the presence and relative concentration of compounds **1**–**7** were examined *in situ* using a droplet-liquid microjunction-surface sampling probe (droplet-LMJ-SSP), followed by analysis via UPLC-PDA-HRMS-MS/MS, all according to a previously described procedure (Sica et al., 2015). Compounds **1**, **2** and/or **4** (as they have the same molecular weight), **3**, **5**, and **6** were detected and identified in the guttate based on their retention times, accurate *m*/*z* match (±5 ppm), and MS/MS fragmentation patterns (Figs. S17–S21). Compound **1** appeared to be the most abundant in *L. madisonensis* (G416), based on its relative intensity compared to **2** and/or **4** and **5**, as shown in Fig. 3C. Although compounds **3** and **6** were identified in the guttate by droplet-LMJ-SSP, they were only present in trace amounts compared to **1**. Compounds **1**, **2** and/or **4**, and trace amounts of **5** were also detected on the outer mycelium of G416; however, in all cases, these compounds were more concentrated in the guttate. It is thus hypothesized that compound **7** was not detected in the culture, either because the fungus biosynthesized it only when grown on rice or after an extended period of time. This result was not surprising, as it is well known that variation of media conditions can alter the biosynthesis of secondary metabolites in fungi (Du et al., 2012, Vandermolen et al., 2013). An alternative hypothesis could be that compound **7** was located inside the mycelium, rather than on the surface (Sica et al., 2014). Overall, the heat profile (Fig. 3C) suggested that relatively higher concentrations of the

compounds were present in the guttate in comparison with the mycelium. This observation suggested that the fungus could be using the guttate as a reservoir to store and/or concentrate secondary metabolites. Moreover, having a higher concentration of **1**, in general, corroborated the more traditional natural products protocols, where **1** was isolated in the highest yield. With the droplet-LMJ-SSP, the spatial distribution and relative concentration of the compounds were evaluated. This method can provide additional useful information into the metabolism of the fungus *in situ,*which cannot be obtained with traditional isolation techniques. Unfortunately, it was not possible to assign a biological activity to these compounds, and thus, their potential role in the fungal life cycle is unknown at this time. Further studies to evaluate the biological relevance of these compounds, particularly in relation to their concentration in guttates, are ongoing.

3. Conclusion

Lindgomycetaceae is a recently described family of freshwater ascomycetes, and little is known about the chemistry produced by species in this family (Hirayama et al., 2010). In a previous study, the fatty acid, 6*E*,9*E*-octadecadienoic acid, and the steroid derivative, ergosterol peroxide, were shown to be the major compounds produced by *Lindgomyces angustiascus* (Raja et al., 2013a). Additionally, strains phylogenetically related to the Lindgomycetaceae, isolated recently from two different marine habitats, produced the newly described compound lindgomycin and ascosetin, both of which have polyketide structures (Wu et al., 2015). The isolation and identification of acetophenone derivatives **1**–**7** from *L. madisonensis* highlights the potential of freshwater ascomycetes as a source of new chemical diversity. The use of droplet-LMJ-SSP demonstrated the concentration of these secondary metabolites in the guttate, suggesting that guttates may serve as a reservoir of secondary metabolites, at least under certain growth conditions.

4. Experimental

4.1. General experimental procedures

The NMR data were collected using either a JEOL ECS-400 spectrometer (JEOL USA, Inc.) operating at 400 MHz for ^{1}H and 100 MHz for ^{13}C, and equipped with JEOL normal geometry broadband Royal probe, or an Agilent 700 MHz NMR spectrometer (Agilent Technologies, Inc., Santa Clara, CA, USA) operating at 700 MHz for ^{1}H and 175 MHz for ^{13}C, and equipped with a cryoprobe. NMR chemical shift values were referenced to residual solvent signals for CD_3OD (δ_H/δ_C 3.31/49.0) and $CDCl_3$ (δ_H/δ_C 7.26/77.2). HRESIMS data were obtained using a Thermo QExactive Plus mass spectrometer (ThermoFisher, San Jose, CA, USA) paired with an electrospray ionization source. Analysis of the fungal culture by *in situ* sampling was performed using the CTC/LEAP HTC PAL autosampler (LEAP Technologies Inc.) converted to an automated droplet-LMJ-SSP by using in-house developed software dropletProbe Premium. The droplet-LMJ-SSP was coupled with a Waters Acquity ultraperformance liquid chromatography (UPLC) system (Waters Corp.) and a Thermo QExactive Plus. The HCD fragmentation used a normalized collision energy of 30 eV for all the compounds to obtain MS/MS data. The UPLC separation was performed using an Acquity BEH C18 column (50 mm × 2.1 mm i.d., 1.7 μm) equilibrated at 40 °C and a flow rate set at 0.3 mL/min. The mobile phase consisted of a linear

$CH_3CN–H_2O$ (acidified with 0.1% HCO_2H) gradient starting at 15% CH_3CN to 100% CH_3CN over 8 min, this being held for another 1.5 min before going back to the starting conditions. HPLC separations were performed using Varian ProStar HPLC system connected to a ProStar 335 photodiode array detector (PDA) with UV detection set at 210 nm and 254 nm. Preparative HPLC purification of isolated compounds was performed on a Phenomenex Synergi 4 μm particle size C_{18} column (21 × 250 mm) at a flow rate of 21.24 mL/min. Flash column chromatography (CC) was carried out with a Teledyne ISCO Combiflash Rf connected to an ELSD and PDA detectors with UV detection set at 200–400 nm. UV data were acquired using a Varian Cary 100 Bio UV–Vis spectrophotometer (Varian Inc., Walnut Creek, CA, USA). IR data were recorded using a Perkin-Elmer Spectrum One with Universal ATR attachment (PerkinElmer, Waltham, MA, USA). Melting point data were determined using an SRS DigiMelt Melting Point Apparatus, MPA 160 (Stanford Research Systems, Inc., Sunnyvale, CA, USA), and are uncorrected.

4.2. Fungal strain isolation and identification

The fungal strain, *L. madisonensis* (G416), was isolated from partially decorticated submerged wood collected from Big Beaver Island creek in Madison, North Carolina, USA (36°27′40.0″N 80°01′46.0″W; water pH: 5; water temp 10 °C). Sample collection and isolations were made using procedures outlined earlier (Shearer et al., 2004). Identification of strain *L. madisonensis* (G416) was accomplished by analysis of molecular sequence data from the nuclear ribosomal internal transcribed spacer region (ITS rDNA). This gene region has been officially designated as the barcoding marker for species identification of fungal strains (Schoch et al., 2012). In addition, portions of the 18S rDNA (partial SSU) and 28S rDNA (partial LSU) were also sequenced using primers NS1 and NS4 for SSU (White et al., 1990) and LROR and LR6 for LSU (Rehner and Samuels, 1995, Vilgalys and Hester, 1990). The DNA extraction, PCR amplification, sequencing protocols, and phylogenetic analysis were accomplished using methods described previously (Figueroa et al., 2014, Raja et al., 2013a). A BLAST search of the ITS sequence from G416 against GenBank suggested that the fungal strain had affinities with members of the freshwater ascomycetes genus *Lindgomyces,* (Lindgomycetaceae, Dothideomycetes, Ascomycota) (Hirayama et al., 2010, Raja et al., 2013a; Raja et al., 2011, Zhang et al., 2014). Based on examination of morphology, and maximum likelihood analyses using portions of the rDNA gene (partial SSU, and partial LSU; Fig. S22), the strain G416 has been identified as new species of *L. madisonensis* Raja & Oberlies (Crous et al., 2015). The ex-holotype cultures (single ascospore isolate from holotype) of the new species have been deposited in the Deutsche Sammlung von Mikroorganismen und Zellkulturen, Germany (DSMZ) as (DSM-100629) and Centraalbureau voor Schimmelcultures, Netherlands (CBS) as (CBS 140367). A voucher culture (accession G416) is also maintained in the Department of Chemistry and Biochemistry culture collection at the University of North Carolina at Greensboro. The sequence data from the newly established species have been deposited in GenBank (SSU: KT207822, KT207823; ITS: KT207818, KT207819; and LSU: KT207820, KT207821).

4.3. Fermentation, extraction, and isolation

The fermentation for *L. madisonensis* (G416) was performed using procedures described previously with slight modifications (El-Elimat et al., 2014a, Kaur et al., 2015). Briefly, a seed

culture of *L. madisonensis* (G416) was grown on a potato dextrose agar (PDA, Difco) slant for about 14 days. Subsequently, a small agar plug with mycelium was inoculated on liquid YESD media, followed by incubation for approximately 14 days at rt with shaking at 125 rpm using a rotary shaker. Once sufficient fungal growth was observed in the seed culture, it was inoculated into four 250 mL Erlenmeyer flask, each containing 30 mL of autoclaved rice medium (consisting of 10 g of rice and deionized H_2O that was twice the volume of rice) and grown at rt for a period of 28 days.

To each solid fermentation culture of *L. madisonensis* (G416), CH_3OH–$CHCl_3$ (60 mL, 1:1) was added, and these were shaken for 16 h on an orbital shaker. The resulting mixtures were filtered under vacuum, and the filtrate from each of the four Erlenmeyer flasks was combined. To the filtrate $CHCl_3$ (360 mL) and H_2O (600 mL) were added, and the mixture was stirred for 30 min and then transferred into a separatory funnel. The organic layer was drawn off and dried *in vacuo*. This dried organic extract was defatted by reconstituting in a mixture of CH_3OH–CH_3CN (400 mL, 1:1) and hexane (400 mL), and then partitioned in a separatory funnel. The CH_3OH-CH_3CN layer was collected and concentrated *in vacuo*. The resulting CH_3OH-CH_3CN extract (428 mg) was then adsorbed on Celite 545, and subjected to silica flash CC on a 12 g RediSep Rf Gold Si-gel column, eluting with an increasing gradient of hexane to $CHCl_3$ at a flow rate of 30 mL/min over 61 column volumes, and for a duration of 34 min to give 48 fractions each containing 22 mL. The resulting fractions were then pooled according to their ELSD and UV profiles, which resulted in five combined fractions in total. All were examined by analytical HPLC, and fractions 1–3 warranted further purification based on their chromatographic profiles.

Fraction 3 (23 mg) was purified further by preparative reversed phase HPLC eluting with a linear gradient from CH_3CN: H_2O containing 0.1% HCO_2H (40:60 → 60:40, v/v) at a flow rate of 21.2 mL/min over 30 min to afford compound **1** (14.5 mg, t_R = 13.3 min). Fraction 2 (17 mg) was purified using the same preparative RP-HPLC conditions yielding compounds **2** (11.7 mg, t_R = 10.4 min) and **6** (1.4 mg, t_R = 26.4 min). Fraction 1 (75 mg) was separated using a linear gradient from 40% to 80% CH_3CN containing 0.1% HCO_2H (40:60 → 80:20, v/v) to give compounds **3** (1.4 mg, t_R = 15.4 min), **4** (0.9 mg, t_R = 13.2 min), **5** (8.1 mg, t_R = 16.6 min), and **7** (0.9 mg, t_R = 23.1 min).

4.3.1. Madisone (1)

White solid; m.p. 174–176 °C; UV (CH_3OH) λ_{max} (log ε) 306 (3.30), 237 (3.25) nm; IR (ATR) ν_{max} 3319, 3012, 2972, 2939, 2754, 1610, 1573, 1449, 1265, 1195, 803 cm^{-1}; ^1H (400 MHz) and ^{13}C NMR (100 MHz) both in CD_3OD, see Table 1; HRESIMS *m*/*z*227.09129 $[M+H]^+$ (calc'd for $C_{11}H_{15}O_5$, 227.09140).

4.3.2. 4′-Methoxymadisone (**2**)

White solid; UV (CH_3OH) λ_{max} (log ε) 293 (3.33), 237 (3.28) nm; IR (ATR) ν_{max} 3275, 3007, 2976, 2940, 2885, 1618, 1579, 1416, 1265, 1122, 866 cm^{-1}; ^1H (400 MHz) and ^{13}C NMR (100 MHz) both in CD_3OD, see Table 1; HRESIMS *m*/*z* 241.10681 $[M + H]^+$ (calc'd for $C_{12}H_{17}O_5$, 241.10705).

4.3.3. Dehydromadisone (**3**)

White solid; UV (CH_3OH) λ_{max} (log ε) 292 (3.27), 231 (3.21) nm; ^1H (400 MHz) and ^{13}C NMR (100 MHz) both in CD_3OD, see Table 1; HRESIMS *m*/*z* 211.09644 $[M+H]^+$ (calc'd for $C_{11}H_{15}O_4$, 211.09648).

4.3.4. 2″-Methoxymadisone (**4**)

White solid; UV (CH_3OH) λ_{max} (log ε) 288 (2.92), 226 (2.95) nm; ^1H (700 MHz) and ^{13}C NMR (175 MHz) both in CD_3OD, see Table 1; HRESIMS *m*/*z* 241.10678 $[M+H]^+$ (calc'd for $C_{12}H_{17}O_5$, 241.10705).

4.3.5. Dihydroallovisnaginone (**5**)

White solid; UV (CH_3OH) λ_{max} (log ε) 307 (3.26), 241 (3.22) nm; IR (ATR) ν_{max} 3106, 2986, 2950, 2908, 2864, 1628, 1594, 1389, 1286, 1242, 1192, 884 cm^{-1}; ^1H (400 MHz) and ^{13}C NMR (100 MHz) both in CD_3OD, see Table 1; HRESIMS *m*/*z* 209.08083$[M+H]^+$ (calc'd for $C_{11}H_{13}O_4$, 209.08083).

4.3.6. Dimadisone (**6**)

White solid; UV (CH_3OH) λ_{max} (log ε) 292 (3.54), 235 (3.49) nm; ^1H (400 MHz) and ^{13}C NMR (100 MHz) both in CD_3OD, see Table 1; HRESIMS *m*/*z* 435.16467 $[M+H]^+$ (calc'd for $C_{22}H_{27}O_9$, 435.16496).

4.3.7. 4′-Methoxydimadisone (**7**)

White solid; UV (CH_3OH) λ_{max} (log ε) 292 (3.60), 231 (3.54) nm; ^1H (700 MHz) and ^{13}C NMR (175 MHz) both in CD_3OD, see Table 2; HRESIMS *m*/*z* 449.18039 $[M+H]^+$ (calc'd for $C_{23}H_{29}O_9$, 449.18061).

4.4. X-ray Crystallography

Crystals of compound **1** were grown in CH_3OH at room temperature. A clear colourless irregular-shaped specimen of $C_{11}H_{14}O_5$, approximate dimensions 0.030 mm × 0.160 mm × 0.290 mm, was used for the X-ray crystallographic analysis. The X-ray intensity data were measured on a Bruker APEX CCD system equipped with a graphite monochromator and a Mo Kα sealed X-ray tube (λ = 0.71073 Å). The total exposure time was 20.70 h. The frames were integrated with the Bruker SAINT software package using a narrow-frame algorithm. The integration of the data using an orthorhombic unit cell yielded a total of 15607 reflections to a maximum θ angle of 30.03° (0.71 Å resolution), of which 3150 were independent (Friedel opposites not merged, average redundancy 4.955, completeness = 99.7%, R_{int} = 4.04%, R_{sig} = 3.01%) and 2720 (86.35%) were greater than $2\sigma(F^2)$. The final cell constants of a = 4.3710(4) Å, b = 11.6045(11) Å, c = 21.2672(19) Å, volume = 1078.74(17) $Å^3$, are based upon the refinement of the *XYZ*-centroids of 4245 reflections above 20 σ (I) with 7.022° < 2θ < 56.44°. Data were corrected for scaling and absorption effects using the multi-scan method (SADABS). The ratio of

minimum to maximum apparent transmission was 0.986. The calculated minimum and maximum transmission coefficients (based on crystal size) are 0.9690 and 0.9970. The structure was solved and refined using the Bruker SHELXTL Software Package, using the space group $P2_12_12_1$, with $Z = 4$ for the formula unit, $C_{11}H_{14}O_5$. The final anisotropic full-matrix least-squares refinement on F^2 with 159 variables converged at $R_1 = 4.22\%$, for the observed data and wR_2 = 10.90% for all data. The goodness-of-fit was 1.031. The largest peak in the final difference electron density synthesis was 0.318 $e^-/Å^3$ and the largest hole was −0.140 $e^-/Å^3$ with an RMS deviation of 0.047 $e^-/Å^3$. On the basis of the final model, the calculated density was 1.393 g/cm^3 and F (0 0 0), 480 e^-. Crystal data, data collection, and structure refinement details are summarized in Table S1.

4.5. Antimicrobial assay

Determination of the minimum inhibitory concentrations (MICs) of compounds **1, 2**, and **5** against *S. aureus*, *E. coli*, *M. smegmatis*, *C. albicans*, and *A. niger* were performed according to previously described methods (Ayers et al., 2012, Williams et al., 2007).

Acknowledgements

We thank Mr. David Sprinkle for permission to collect samples on his property, Dr. Joe Falkinham (Virginia Polytechnic Institute and State University) for the *in vitro* antibacterial and antifungal testing of the isolated compounds, Dr. Tamam El-Elimat (University of North Carolina at Greensboro; UNCG) for helpful suggestions, and Drs. Vilmos Kertesz and Gary J. Van Berkel (Mass Spectrometry and Laser Spectroscopy Group, Chemical Sciences Division, Oak Ridge National Laboratory) for inspiration and guidance with the droplet-LMJ-SSP. The high resolution mass spectrometry data were collected at the Triad Mass Spectrometry Laboratory at UNCG. The Wake Forest University *X*–ray Facility thanks the National Science Foundation (grant CHE–0234489) for funds to purchase the *X*–ray instrument and computers.

Supplementary data

Supplementary data may be found at the end of this formatted document.

References

Aly, A., Debbab, A., Proksch, P., 2011. Fifty years of drug discovery from fungi. Fungal Divers 50, 3–19.

Ayers, S., Ehrmann, B.M., Adcock, A.F., Kroll, D.J., Carcache de Blanco, E.J., Shen, Q., Swanson, S.M., Falkinham 3rd, J.O., Wani, M.C., Mitchell, S.M., Pearce, C.J., Oberlies, N.H., 2012. Peptaibols from two unidentified fungi of the order Hypocreales with cytotoxic, antibiotic, and anthelmintic activities. J. Pept. Sci. 18, 500–510.

Blackwell, M., 2011. The fungi: 1, 2, 3 . . . 5.1 million species? Am. J. Bot. 98, 426–438.

Crous, P.W., Wingfield, M.J., Le Roux, J.J., Richardson, D.M., Strasberg, D., Shivas, R.G., Alvarado, P., Edwards, J., Moreno, G., Sharma, R., Sonawane, M.S., Tan, Y.P., Altés, A., Barasubiye, B., Barnes, C.W., Blanchette, R.A., Boertmann, D., Bogo, A., Carlavilla, J.R., Cheewangkoon, R., Daniel, R., de Beer, Z.W., de Jesús Yáñez-Morales, M., Duong, T.A., Fernández-Vicente, J., Geering, A.D.W., Guest, D.I., Held, B.W., Heykoop, M., Hubka, V., Ismail, A.M., Kajale, S., Khemmuk, W., Kolarˇík, M., Kurli, R., Lebeuf, R., Lévesque, C.A., Lombard, L., Magista, D., Manjón, J.L., Marincowitz, S., Mohedano, J.M., Nováková, A., Oberlies, N.H., Otto, E.C., Paguigan, N.D., Pascoe, I.G., Pérez-Butrón, J.L., Perrone, G., Rahi, P., Raja, H.A., Rintoul, T., Sanhueza, R.M.V., Scarlett, K., Shouche, Y.S., Shuttleworth, L.A., Taylor, P.W.J., Thorn, R.G., Vawdrey, L.L., Vidal, R.S., Voitk, A., Wong, P.T.W., Wood, A.R., Zamora, J.C., Groenewald, J.Z., 2015. Fungal planet description sheets: 371–399. Persoonia 35, 264–327.

Du, L., King, J.B., Morrow, B.H., Shen, J.K., Miller, A.N., Cichewicz, R.H., 2012. Diarylcyclopentendione metabolite obtained from a Preussia typharum isolate procured using an unconventional cultivation approach. J. Nat. Prod. 75, 1819–1823.

El-Elimat, T., Raja, H.A., Day, C.S., Chen, W.L., Swanson, S.M., Oberlies, N.H., 2014a. Greensporones: resorcylic acid lactones from an aquatic Halenospora sp. J. Nat. Prod. 77, 2088–2098.

El-Elimat, T., Raja, H.A., Figueroa, M., Falkinham 3rd, J.O., Oberlies, N.H., 2014b. Isochromenones, isobenzofuranone, and tetrahydronaphthalenes produced by Paraphoma radicina, a fungus isolated from a freshwater habitat. Phytochemistry 104, 114–120.

Figueroa, M., Jarmusch, A.K., Raja, H.A., El-Elimat, T., Kavanaugh, J.S., Horswill, A.R., Cooks, R.G., Cech, N.B., Oberlies, N.H., 2014. Polyhydroxyanthraquinones as quorum sensing inhibitors from the guttates of Penicillium restrictum and their analysis by desorption electrospray ionization mass spectrometry. J. Nat. Prod. 77, 1351–1358.

Gareis, M., Gareis, E.-M., 2007. Guttation droplets of Penicillium nordicum and Penicillium verrucosum contain high concentrations of the mycotoxins ochratoxin A and B. Mycopathologia 163, 207–214.

Geissman, T.A., Hinreiner, E., 1951. Chromones. II. The synthesis of visnaginone. J. Am. Chem. Soc. 73, 782–786.

Hernández-Carlos, B., Gamboa-Angulo, M.M., 2011. Metabolites from freshwater aquatic microalgae and fungi as potential natural pesticides. Phytochem. Rev. 10, 261–286.

Hirayama, K., Tanaka, K., Raja, H.A., Miller, A.N., Shearer, C.A., 2010. A molecular phylogenetic assessment of Massarina ingoldiana sensu lato. Mycologia 102, 729–746.

Hosoe, T., Gloer, J.B., Wicklow, D.T., Raja, H.A., Shearer, C.A., 2010. New nonadride analogues from a freshwater isolate of an undescribed fungus belonging to the order pleosporales. Heterocycles 81, 2123–2130.

Jiao, P., Swenson, D.C., Gloer, J.B., Campbell, J., Shearer, C.A., 2006. Decaspirones A-E, bioactive spirodioxynaphthalenes from the freshwater aquatic fungus Decaisnella thyridioides. J. Nat. Prod. 69, 1667–1671.

Kaur, A., Raja, H.A., Darveaux, B.A., Chen, W.L., Swanson, S.M., Pearce, C.J., Oberlies, N.H., 2015. New diketopiperazine dimer from a filamentous fungal isolate of Aspergillus sydowii. Magn. Reson. Chem. 53, 616–619.

Li, C., Nitka, M.V., Gloer, J.B., Campbell, J., Shearer, C.A., 2003. Annularins A-H: new polyketide metabolites from the freshwater aquatic fungus Annulatascus triseptatus. J. Nat. Prod. 66, 1302–1306.

Mudur, S.V., Swenson, D.C., Gloer, J.B., Campbell, J., Shearer, C.A., 2006. Heliconols AC: antimicrobial hemiketals from the freshwater aquatic fungus Helicodendron giganteum. Org. Lett. 8, 3191–3194.

Oh, H., Kwon, T.O., Gloer, J.B., Marvanova, L., Shearer, C.A., 1999. Tenellic acids A-D: new bioactive diphenyl ether derivatives from the aquatic fungus Dendrospora tenella. J. Nat. Prod. 62, 580–583.

Raja, H.A., El-Elimat, T., Oberlies, N.H., Shearer, C.A., Tanaka, K., Hoshimoto, A., Fournier, J., 2015. Minutisphaerales (Dothideomycetes, Ascomycota): a new order of freshwater ascomycetes including a new family, Minutisphaeraceae, and two new species from North Carolina, USA. Mycologia 107, 845–862.

Raja, H.A., Oberlies, N.H., El-Elimat, T., Miller, A.N., Zelski, S.E., Shearer, C.A., 2013a. Lindgomyces angustiascus, (Lindgomycetaceae, Pleosporales, Dothideomycetes), a new lignicolous species from freshwater habitats in the USA. Mycoscience 54, 353–361.

Raja, H.A., Oberlies, N.H., Figueroa, M., Tanaka, K., Hirayama, K., Hashimoto, A., Miller, A.N., Zelski, S.E., Shearer, C.A., 2013b. Freshwater ascomycetes: Minutisphaera (Dothideomycetes) revisited, including one new species from Japan. Mycologia 105, 959–976.

Raja, H.A., Tanaka, K., Hirayama, K., Miller, A.N., Shearer, C.A., 2011. Freshwater ascomycetes: two new species of Lindgomyces (Lindgomycetaceae, Pleosporales, Dothideomycetes) from Japan and USA. Mycologia 103, 1421–1432.

Reategui, R.F., Gloer, J.B., Campbell, J., Shearer, C.A., 2005. Ophiocerins A-D and ophioceric acid: tetrahydropyran derivatives and an africane sesquiterpenoid from the freshwater aquatic fungus Ophioceras venezuelense. J. Nat. Prod. 68, 701–705.

Rehner, S.A., Samuels, G.J., 1995. Molecular systematics of the Hypocreales: a teleomorph gene phylogeny and the status of their anamorphs. Can. J. Bot. 73, 816–823.

Schoch, C.L., Seifert, K.A., Huhndorf, S., Robert, V., Spouge, J.L., Levesque, C.A., Chen, W., 2012. Nuclear ribosomal internal transcribed spacer (ITS) region as a universal DNA barcode marker for fungi. Proc. Natl. Acad. Sci. U.S.A. 109, 6241–6246.

Shearer, C.A., 1993. The freshwater Ascomycetes. Nova Hedwigia 56, 1–33.

Shearer, C.A., 2001. The Distribution of Freshwater Filamentous Ascomycetes. Science Publishers, Plymouth, UK, pp. 225–292.

Shearer, C.A., 2007. Fungal biodiversity in aquatic habitats. Biodivers. Conserv. 16, 49–67.

Shearer, C.A., Langsam, D.M., Longcore, J.E., 2004. Fungi in freshwater habitats. In: Mueller, G.M., Bills, G.F., Foster, M.S. (Eds.), Measuring and Monitoring Biological Diversity: Standard Methods for Fungi. Smithsonian Institution Press, Washington, D.C., pp. 513–531.

Shearer, C.A., Raja, H.A., 2015. Freshwater Ascomycetes Database, http://fungi.life.illinois.edu/ (Accessed on April 4, 2015).

Sica, V.P., Raja, H.A., El-Elimat, T., Kertesz, V., Van Berkel, G.J., Pearce, C.J., Oberlies, N.H., 2015. Dereplicating and spatial mapping of secondary metabolites from fungal cultures in situ. J. Nat. Prod. 78, 1926–1936.

Sica, V.P., Raja, H.A., El-Elimat, T., Oberlies, N.H., 2014. Mass spectrometry imaging of secondary metabolites directly on fungal cultures. RSC Adv. 4, 63221–63227.

Vandermolen, K.M., Raja, H.A., El-Elimat, T., Oberlies, N.H., 2013. Evaluation of culture media for the production of secondary metabolites in a natural products screening program. AMB Exp. 3, 71.

Vilgalys, R., Hester, M., 1990. Rapid genetic identification and mapping of enzymatically amplified ribosomal DNA from several Cryptococcus species. J. Bacteriol. 172, 4238–4246.

Wang, X., Sena Filho, J.G., Hoover, A.R., King, J.B., Ellis, T.K., Powell, D.R., Cichewicz, R.H., 2010. Chemical epigenetics alters the secondary metabolite composition of guttate excreted by an atlantic-forest-soil-derived Penicillium citreonigrum. J. Nat. Prod. 73, 942–948.

White, T.J., Bruns, T., Lee, S., Taylor, J., 1990. Amplification and direct sequencing of fungal ribosomal RNA genes for phylogenetics. In: Innis, M., Gelfand, D., Shinsky, J., White, T. (Eds.), PCR Protocols: A Guide to Methods and Applications. Academic Press, pp. 315–322.

Williams, A.A., Sugandhi, E.W., Macri, R.V., Falkinham 3rd, J.O., Gandour, R.D., 2007. Antimicrobial activity of long-chain, water-soluble, dendritic tricarboxylato amphiphiles. J. Antimicrob. Chemother. 59, 451–458.

Wootton, R.C.R., 2000. Synthetic Approaches to Polyoxygenated Chromone and Chromanone Natural Products (Doctoral dissertation). School of Computing, Science and Engineering. University of Salford, UK, p. 222.

Wu, B., Wiese, J., Labes, A., Kramer, A., Schmaljohann, R., Imhoff, J.F., 2015. Lindgomycin, an unusual antibiotic polyketide from a marine fungus of the Lindgomycetaceae. Mar. Drugs 13, 4617–4632.

Zhang, Y., Zhang, X., Fournier, J., Chen, J., Hyde, K.D., 2014. Lindgomyces griseosporus, a new aquatic ascomycete from Europe including new records. Mycoscience 55, 43–48.

Appendix A. Supplementary data

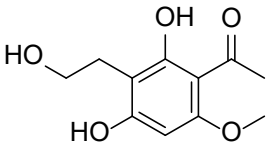

madisone (**1**)

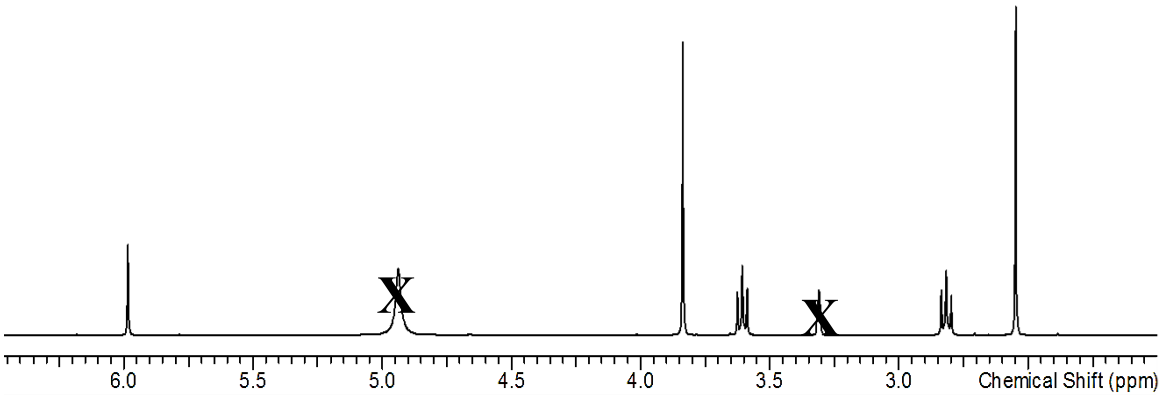

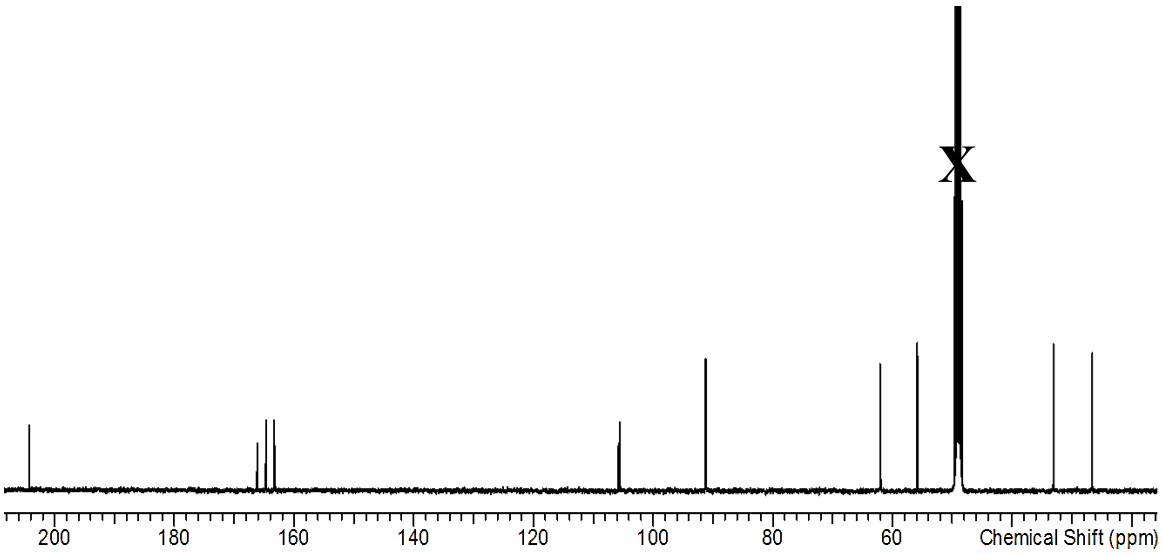

Figure S1. ^{1}H NMR (400 MHz; top) and ^{13}C NMR (100 MHz; bottom) spectra of madisone (**1**) in CD_3OD.

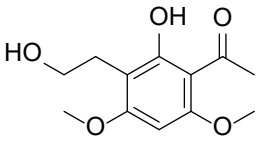

4´-methoxymadisone (**2**)

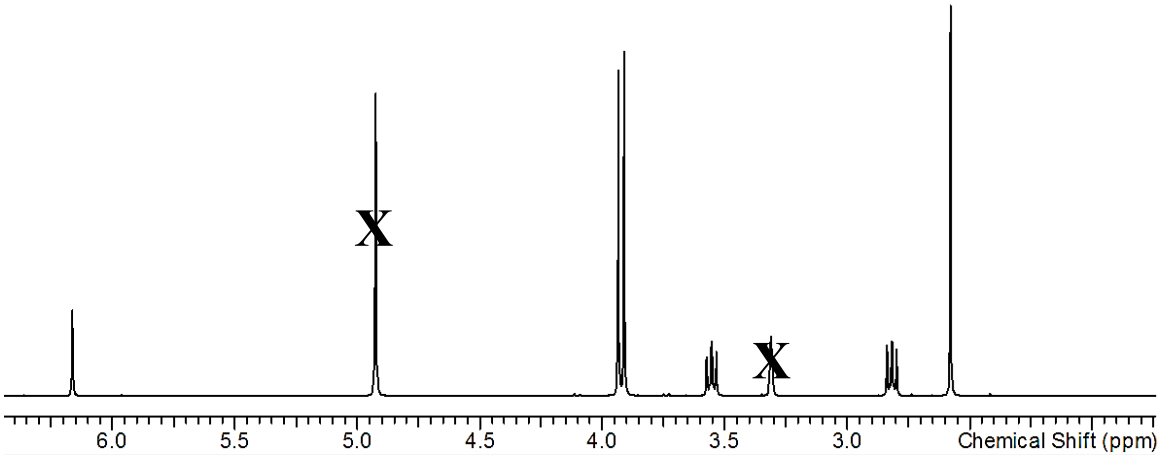

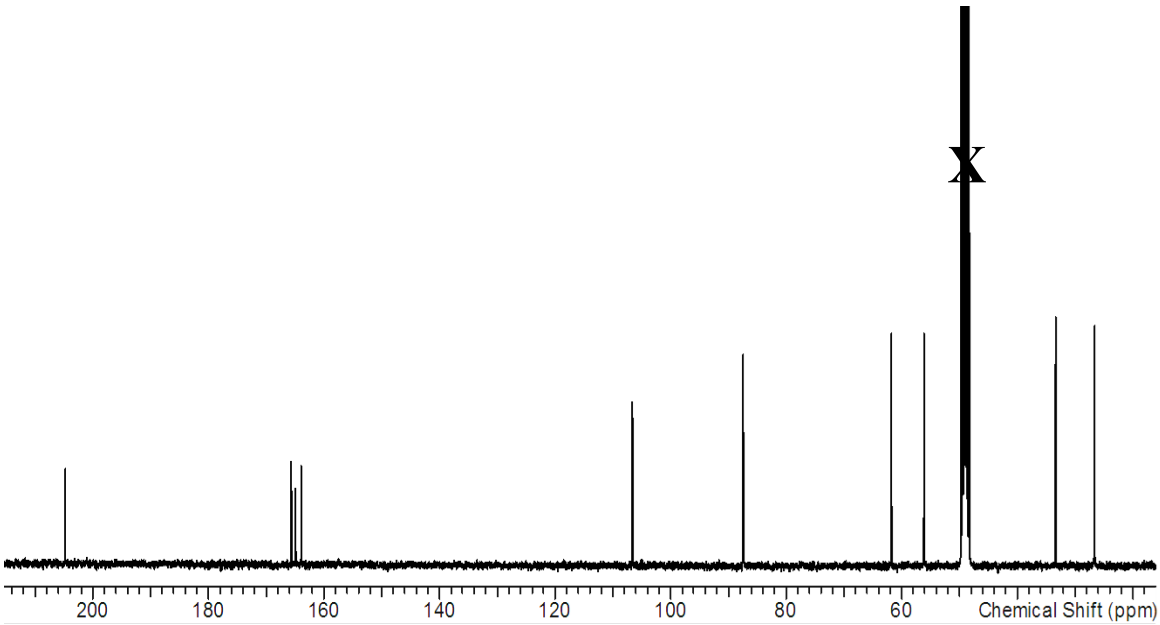

Figure S2. ^{1}H NMR (400 MHz; top) and ^{13}C NMR (100 MHz; bottom) spectra of 4´-methoxymadisone (**2**) in CD_3OD.

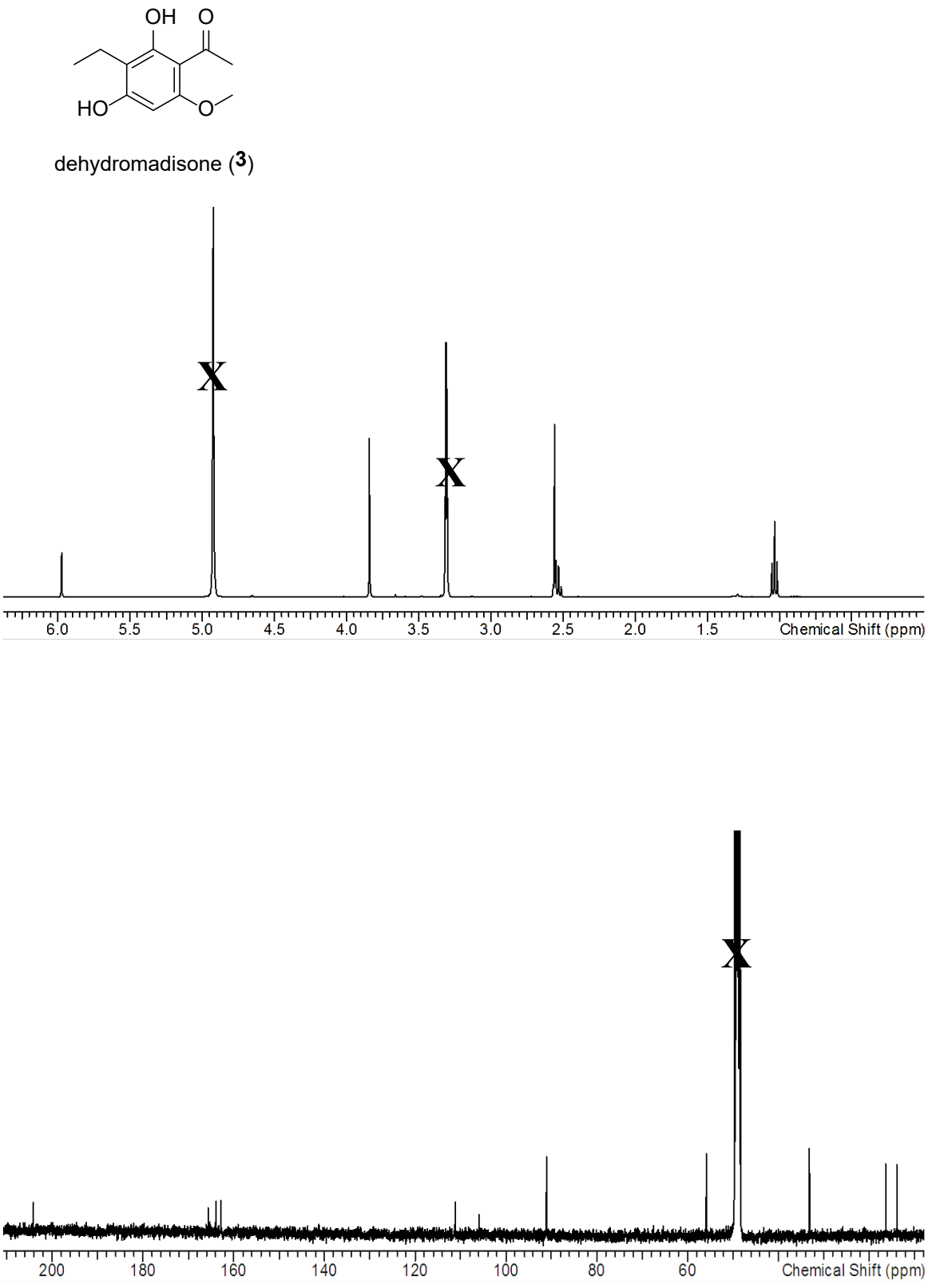

Figure S3. ^{1}H NMR (400 MHz; top) and ^{13}C NMR (100 MHz; bottom) spectra of dehydromadisone (**3**) in CD_3OD.

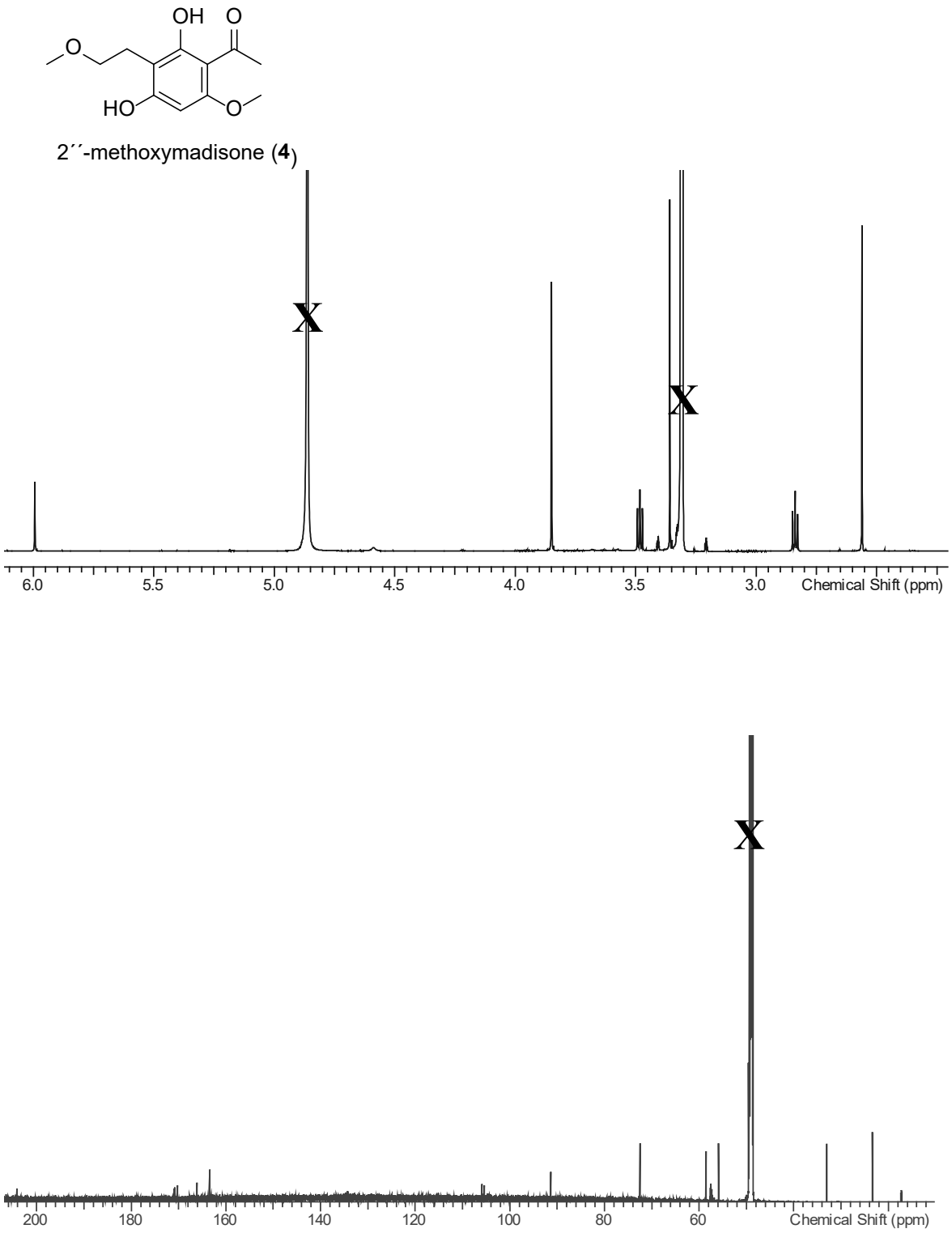

Figure S4. ^{1}H NMR (700 MHz; top) and ^{13}C NMR (175 MHz; bottom) spectra of 2´´-methoxymadisone (**4**) in CD_3OD.

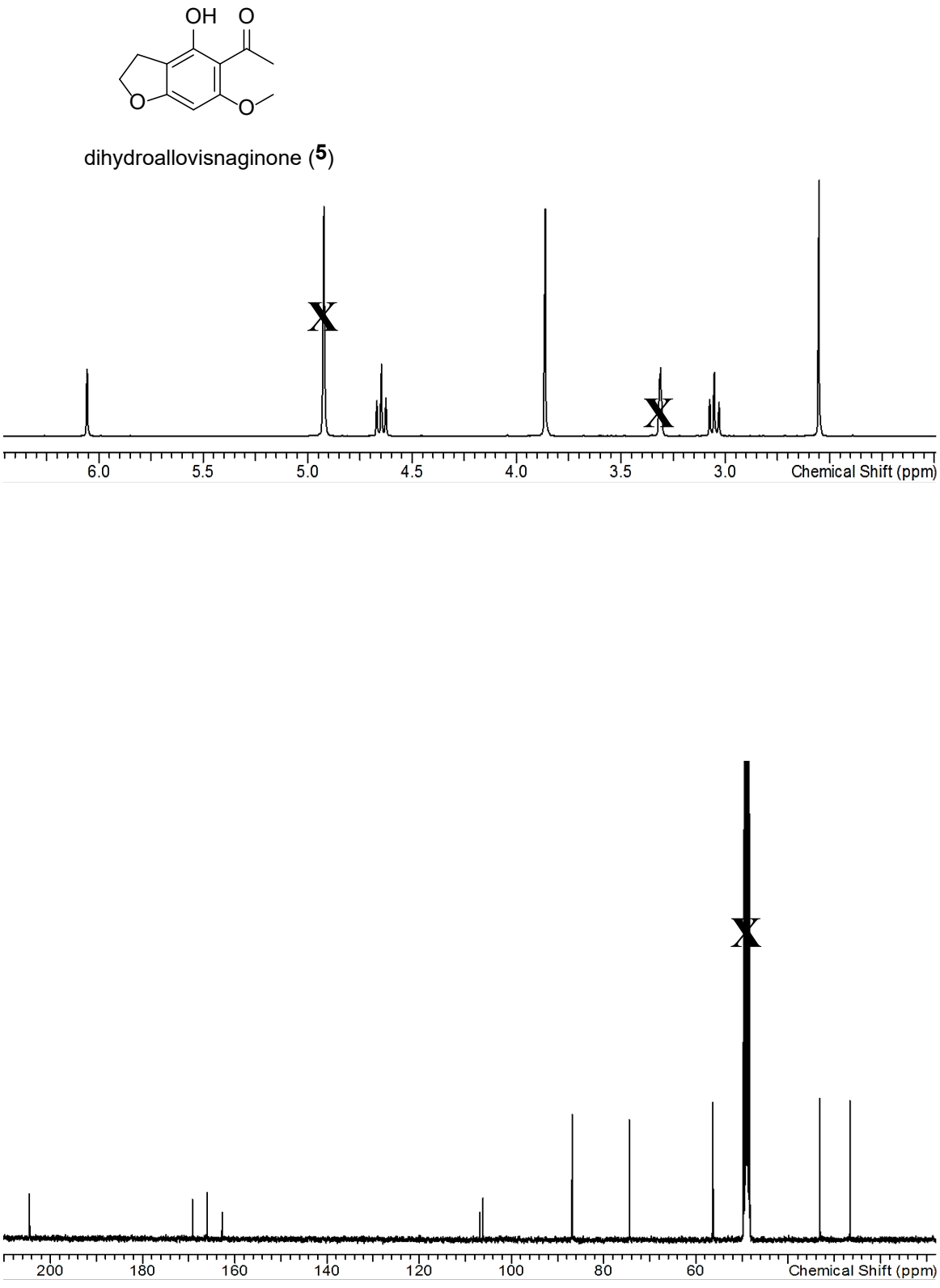

Figure S5. ^{1}H NMR (400 MHz; top) and ^{13}C NMR (100 MHz; bottom) spectra of dihydroallovisnaginone (**5**) in CD_3OD.

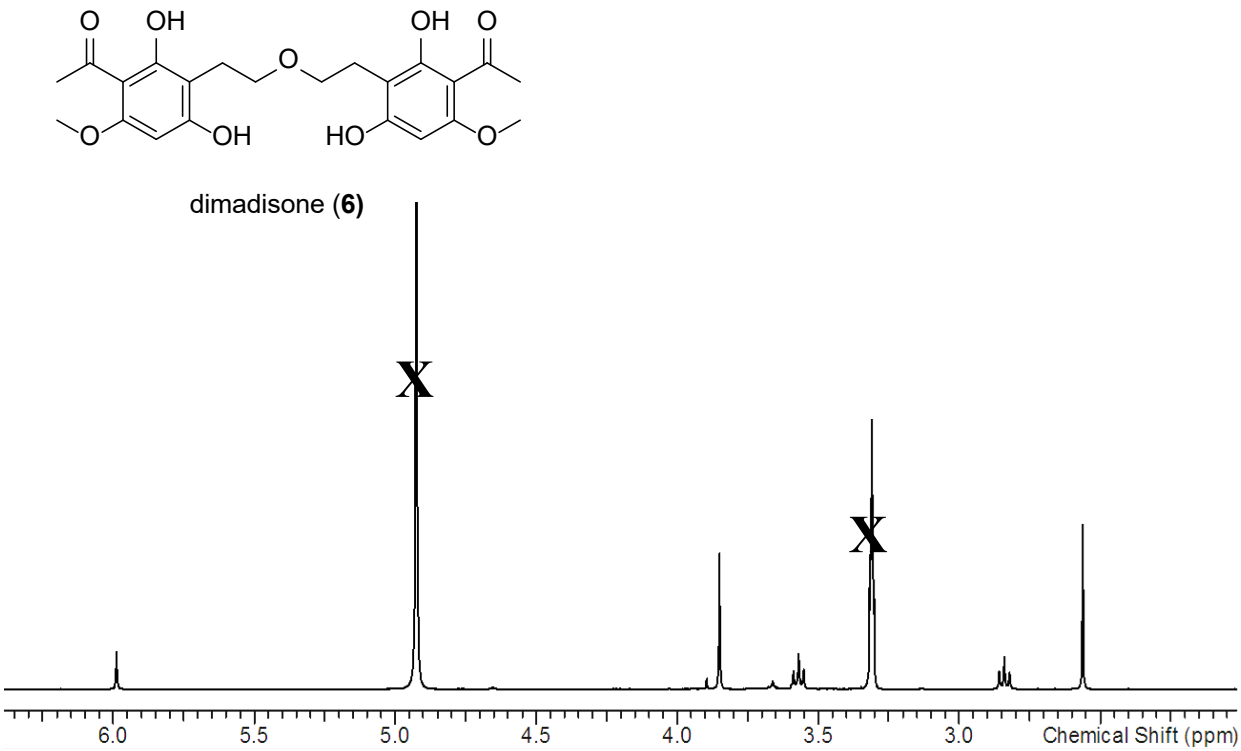

Figure S6. ^{1}H NMR (400 MHz; top) and ^{13}C NMR (100 MHz; bottom) spectra of dimadisone (**6**) in CD_3OD.

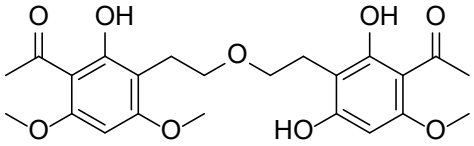

4´-methoxydimadisone (**7**)

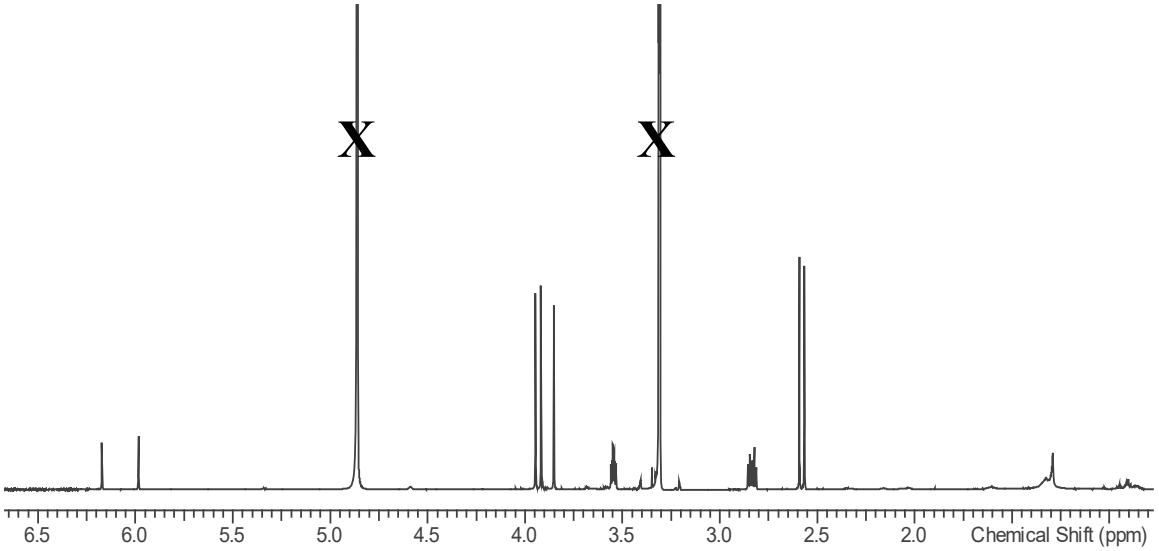

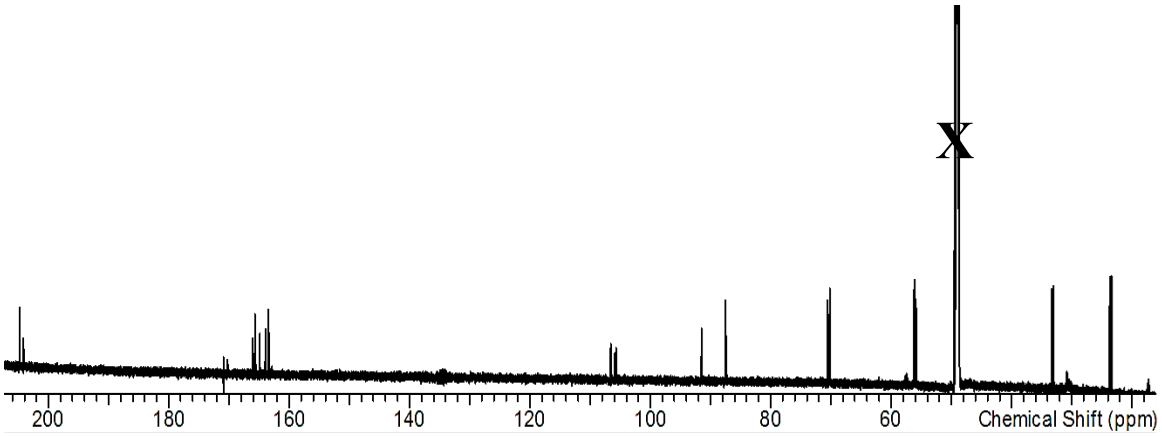

Figure S7. ^{1}H NMR (700 MHz; top) and ^{13}C NMR (175 MHz; bottom) spectra of 4´-methoxydimadisone (**7**) in CD_3OD.

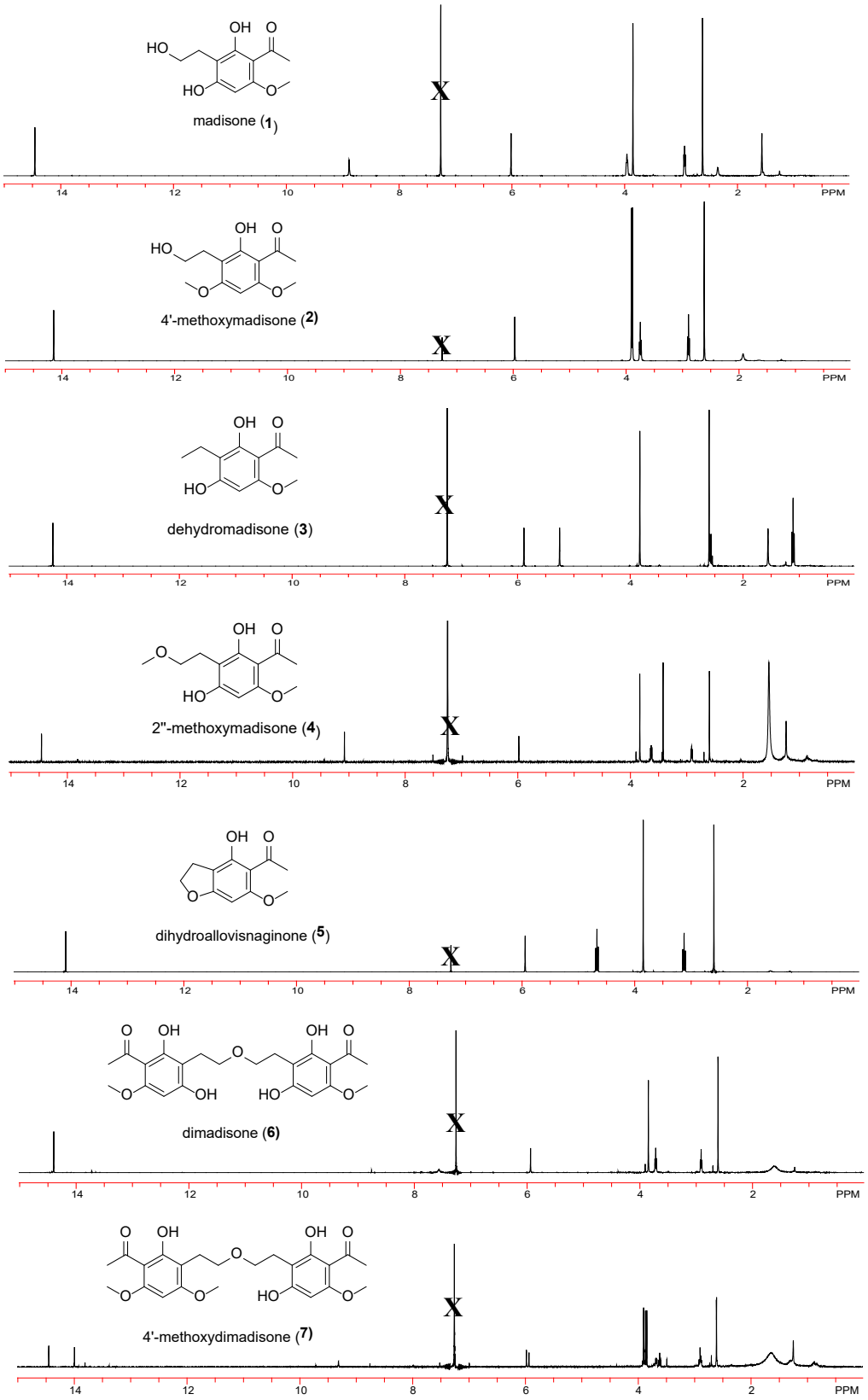

Figure S8. ^{1}H NMR (400 MHz) spectra of compounds **1**-**7** in $CDCl_3$.

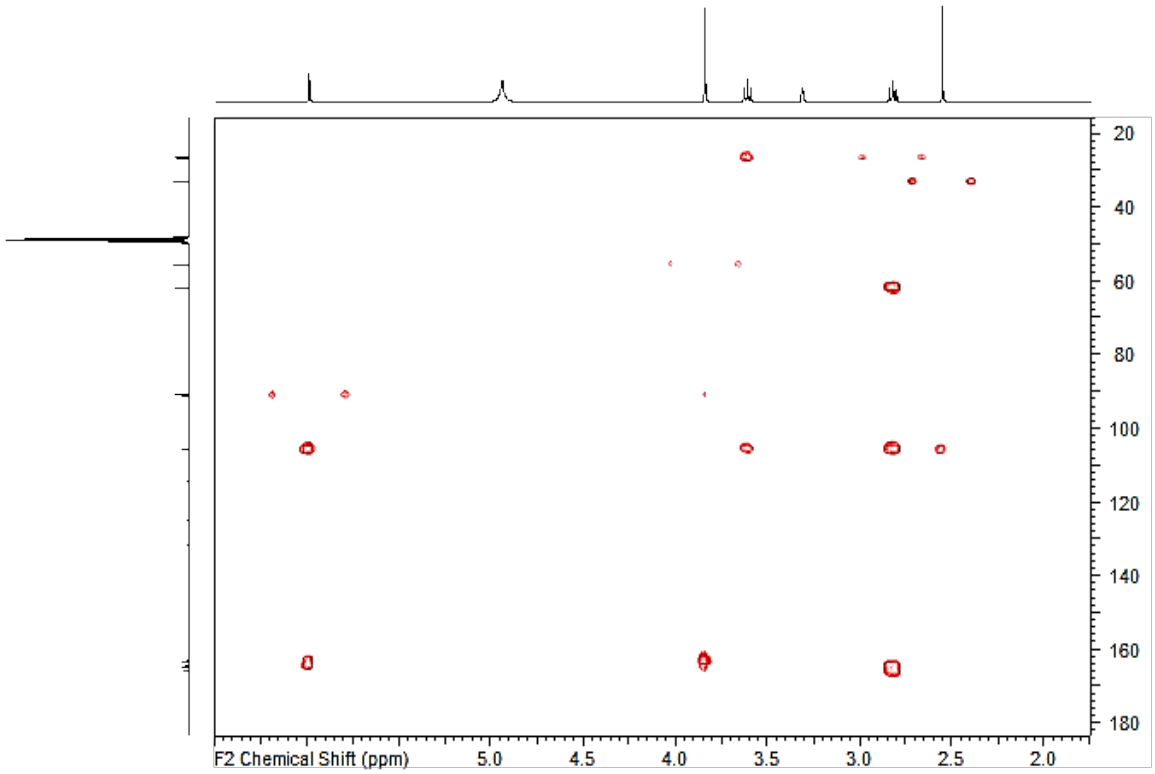

Figure S9. The HMBC (400 MHz/100 MHz) spectrum of madisone (**1**) in CD_3OD.

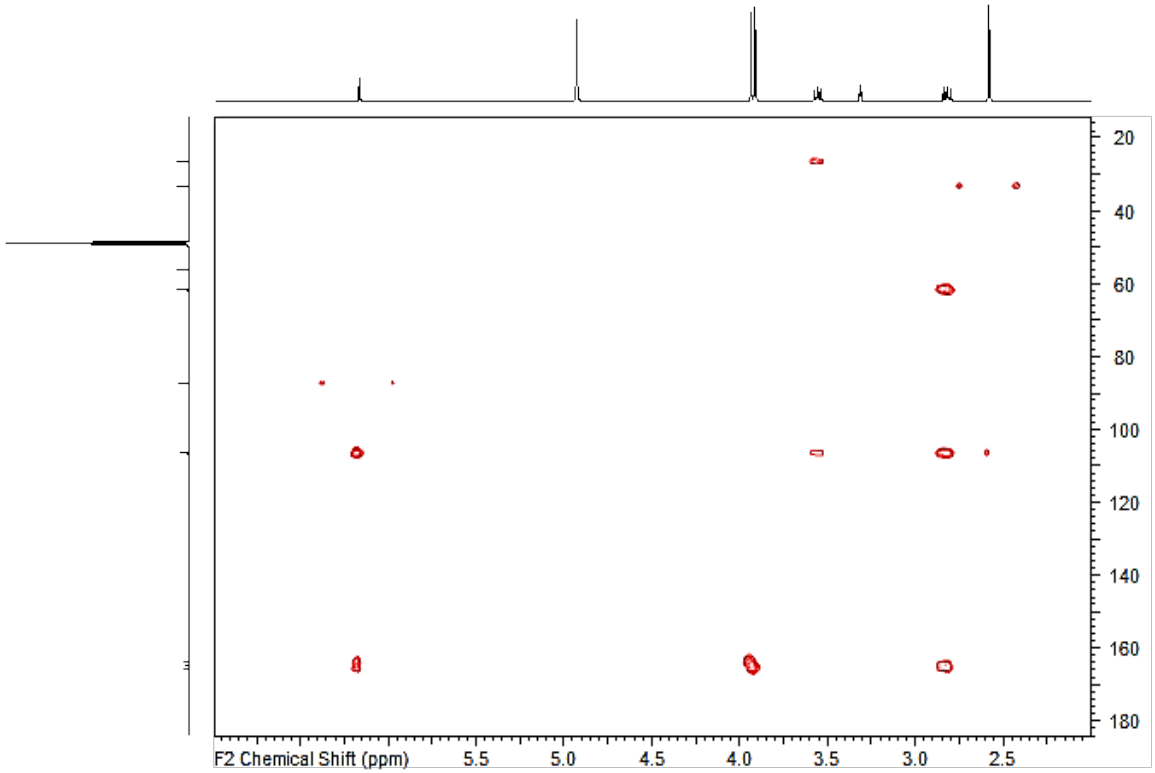

Figure S10. The HMBC (400 MHz/100 MHz) spectrum of 4′-methoxymadisone (**2**) in CD_3OD.

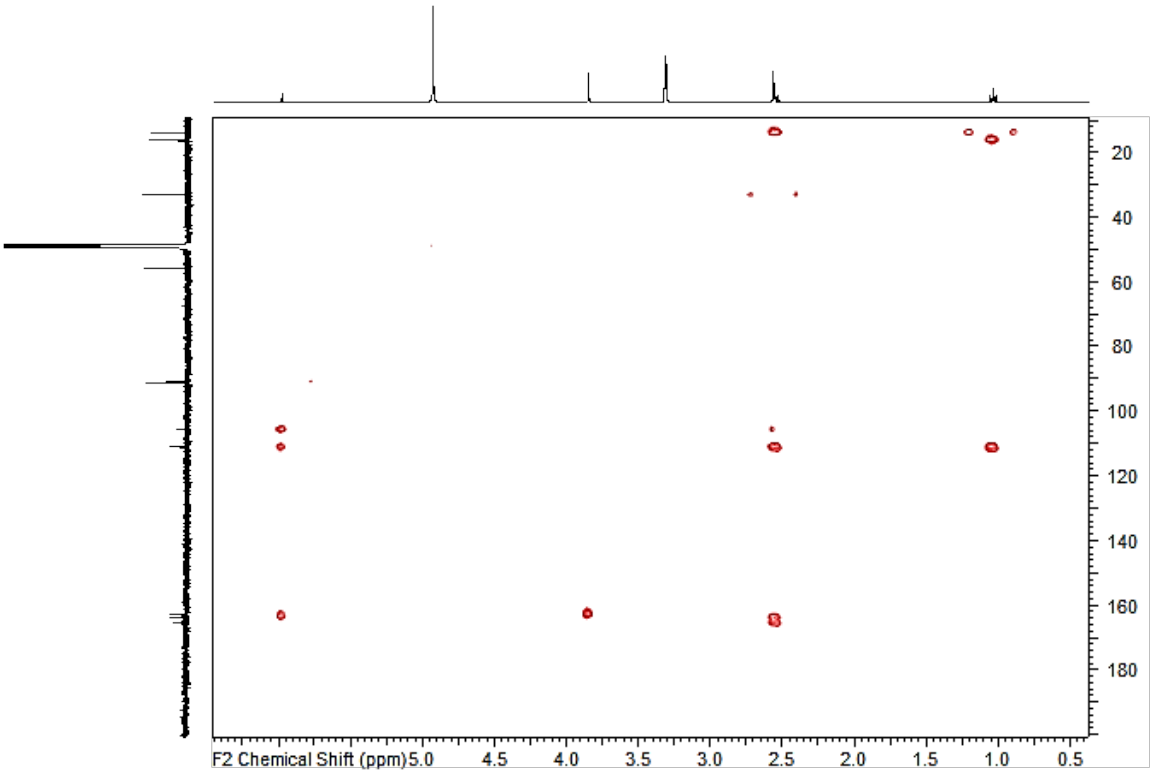

Figure S11. The HMBC (400 MHz/100 MHz) spectrum of dehydromadisone (**3**) in CD_3OD.

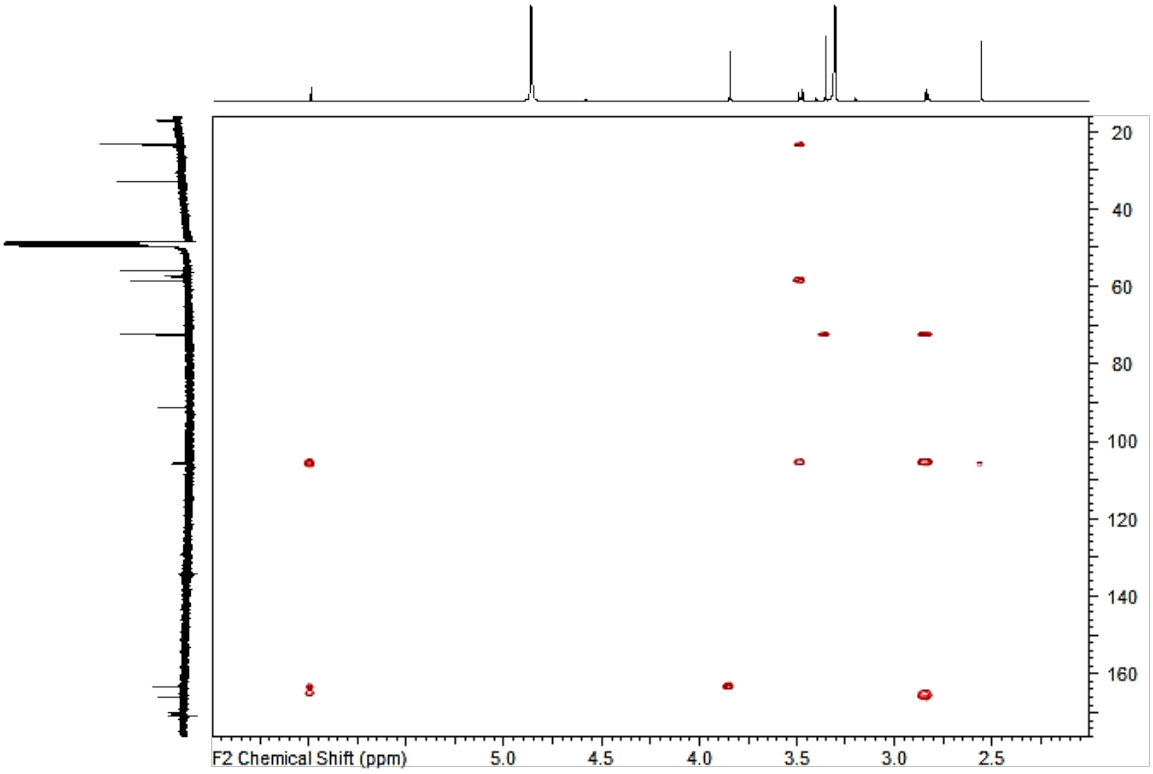

Figure S12. The HMBC (700 MHz/175 MHz) spectrum of 2′′-methoxymadisone (**4**) in CD_3OD.

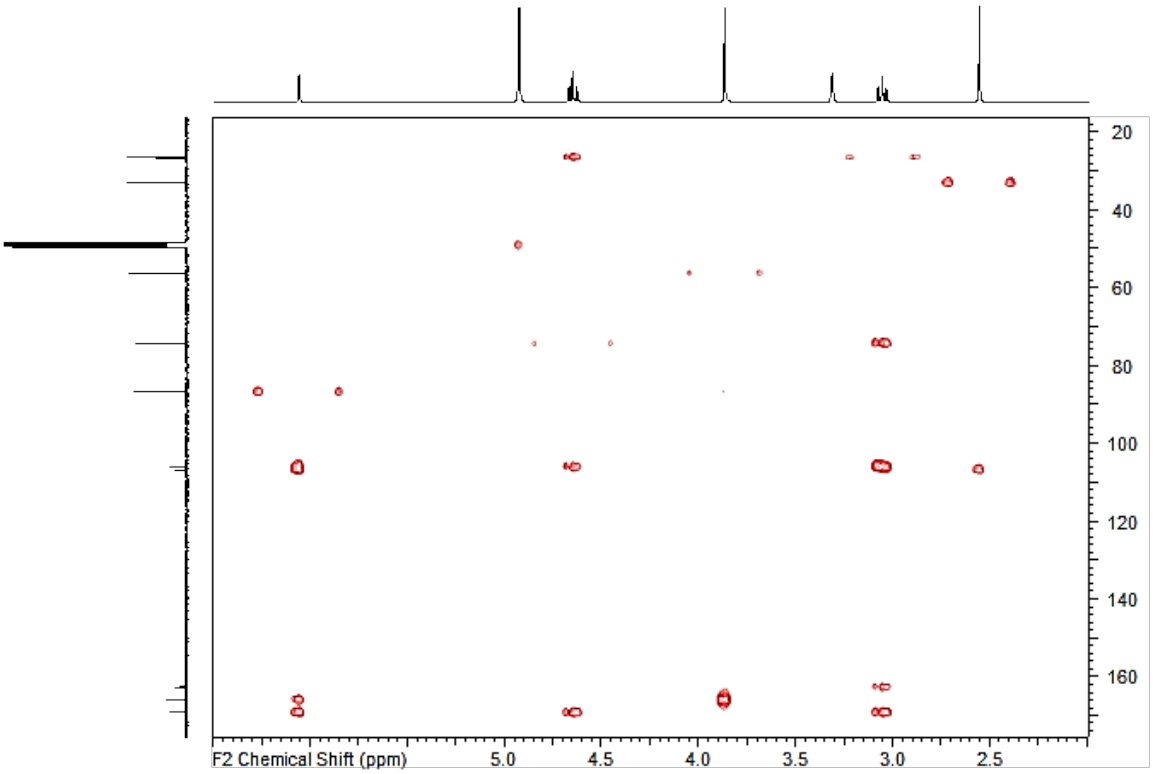

Figure S13. The HMBC (400 MHz/100 MHz) spectrum of dihydroallovisnaginone (**5**) in CD_3OD.

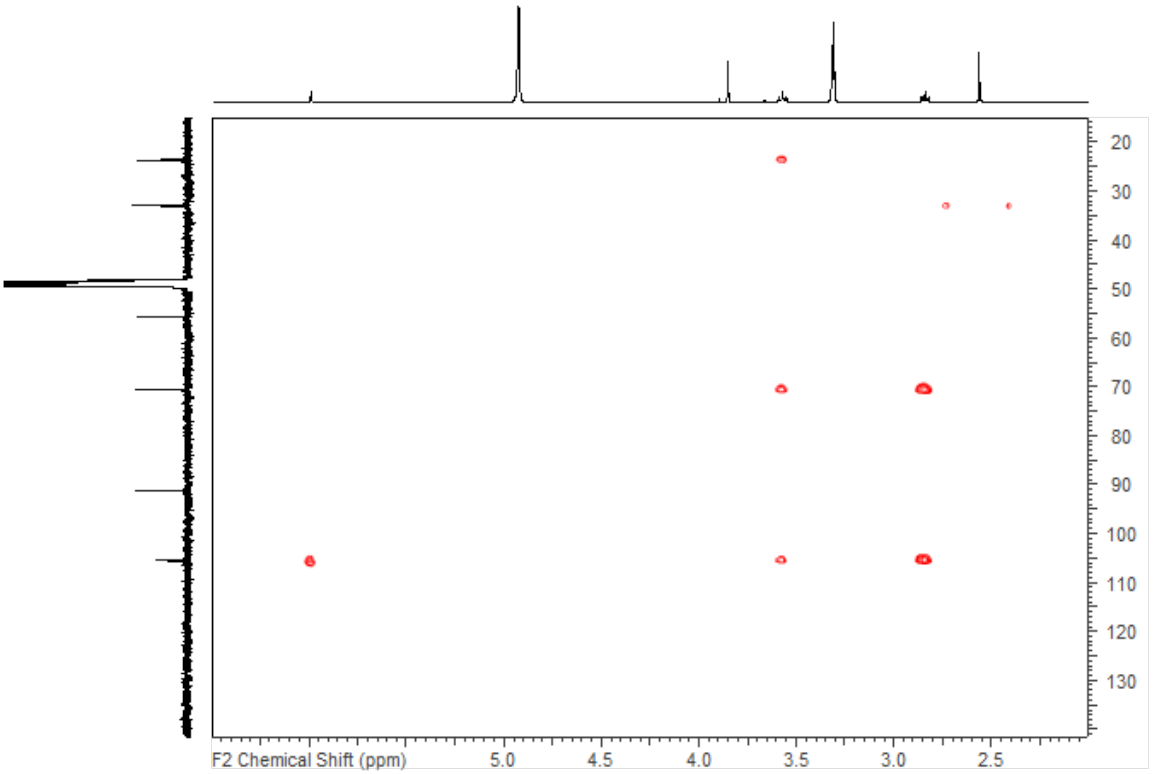

Figure S14. The HMBC (400 MHz/100 MHz) spectrum of dimadisone (**6**) in CD_3OD.

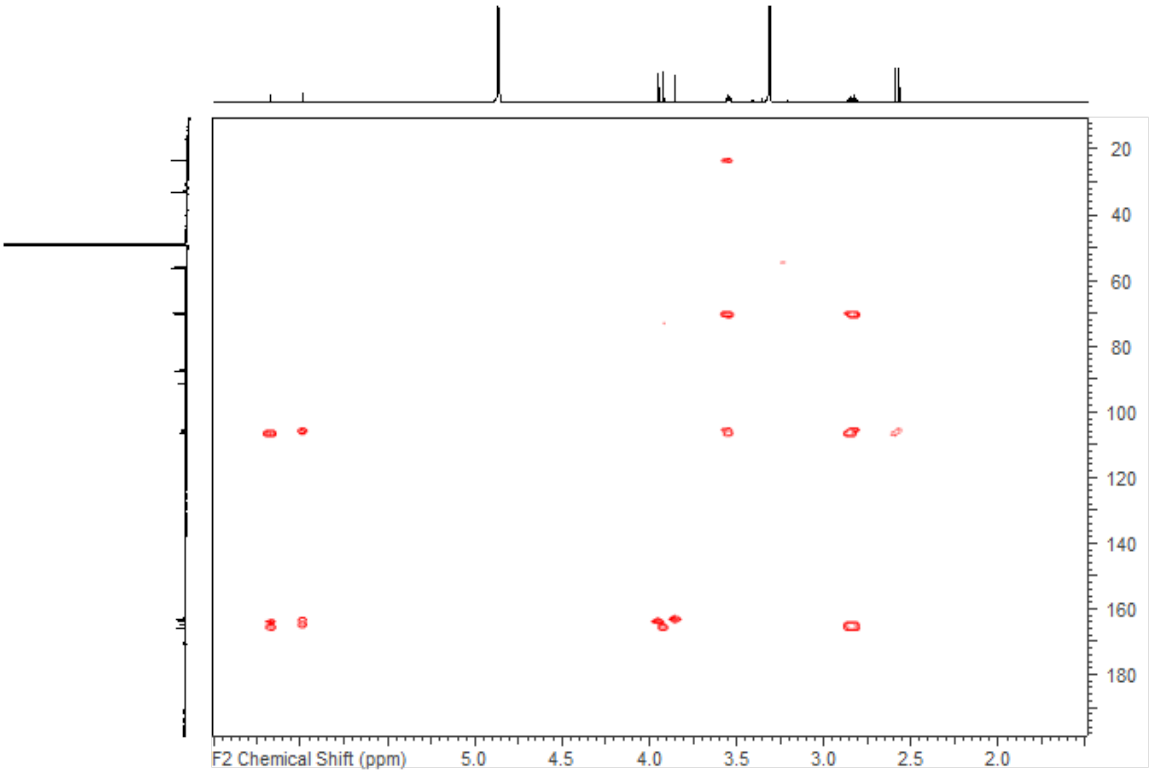

Figure S15. The HMBC (700 MHz/175 MHz) spectrum of 4′-methoxydimadisone (**7**) in CD_3OD.

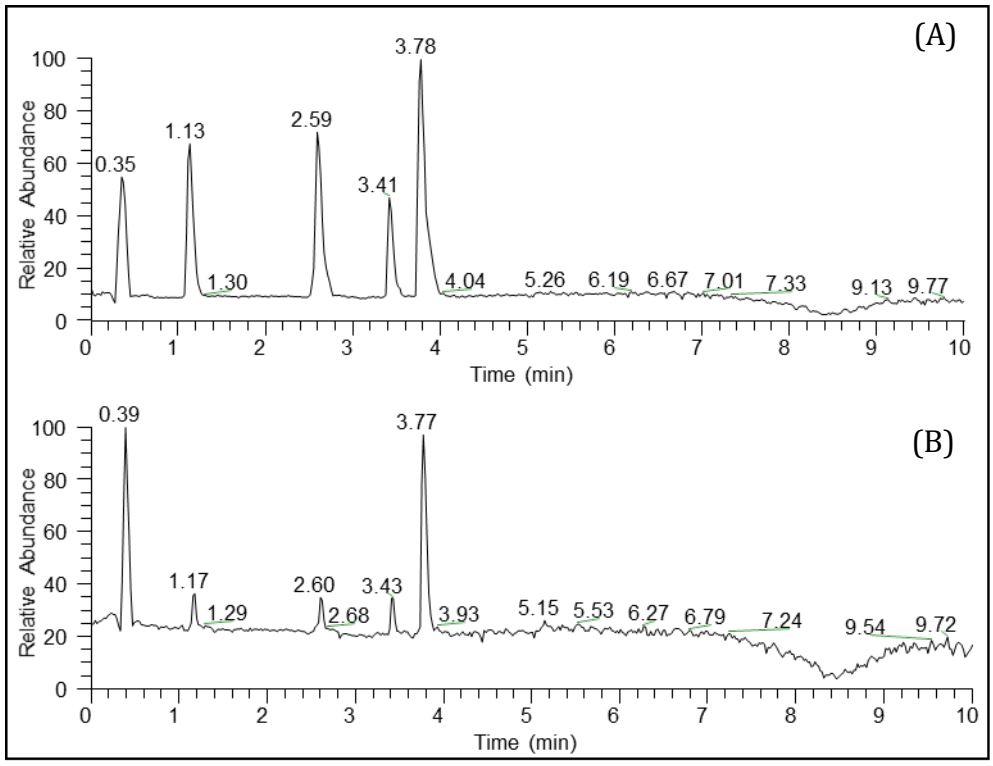

Figure S16. Base peak chromatograms for G416 sampled by the droplet-LMJ-SSP. (A) Guttate produced by G416 (B) Outer mycelium of G416.

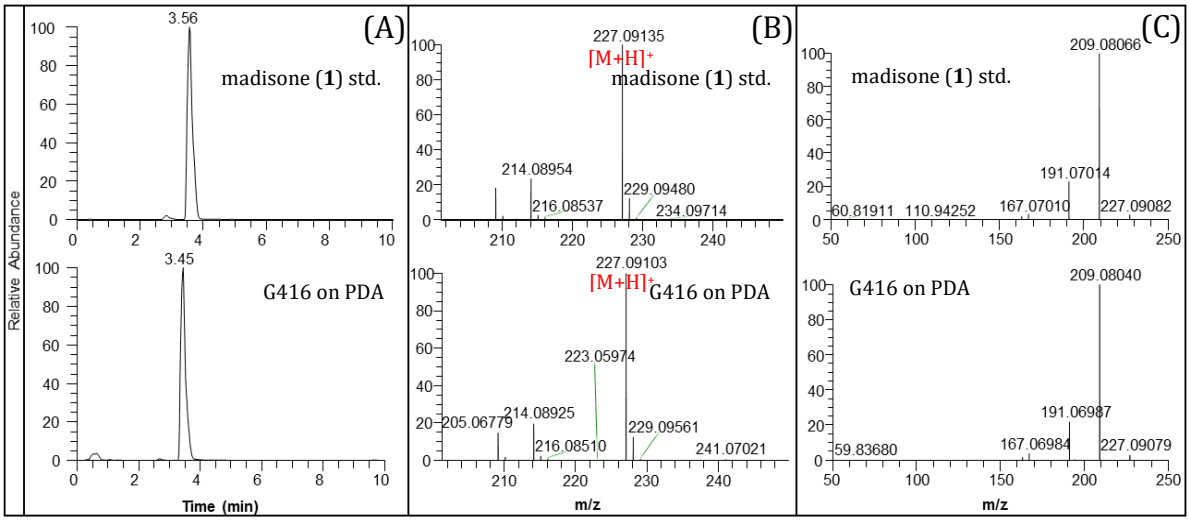

Figure S17. (A) Overlay of chromatographic peaks of **1** (B) (+)-HRESIMS of **1** (C) MS/MS HCD fragmentation of **1.** The top and bottom show the data for the reference standard and *in situ* analysis of G416 grown on PDA, respectively.

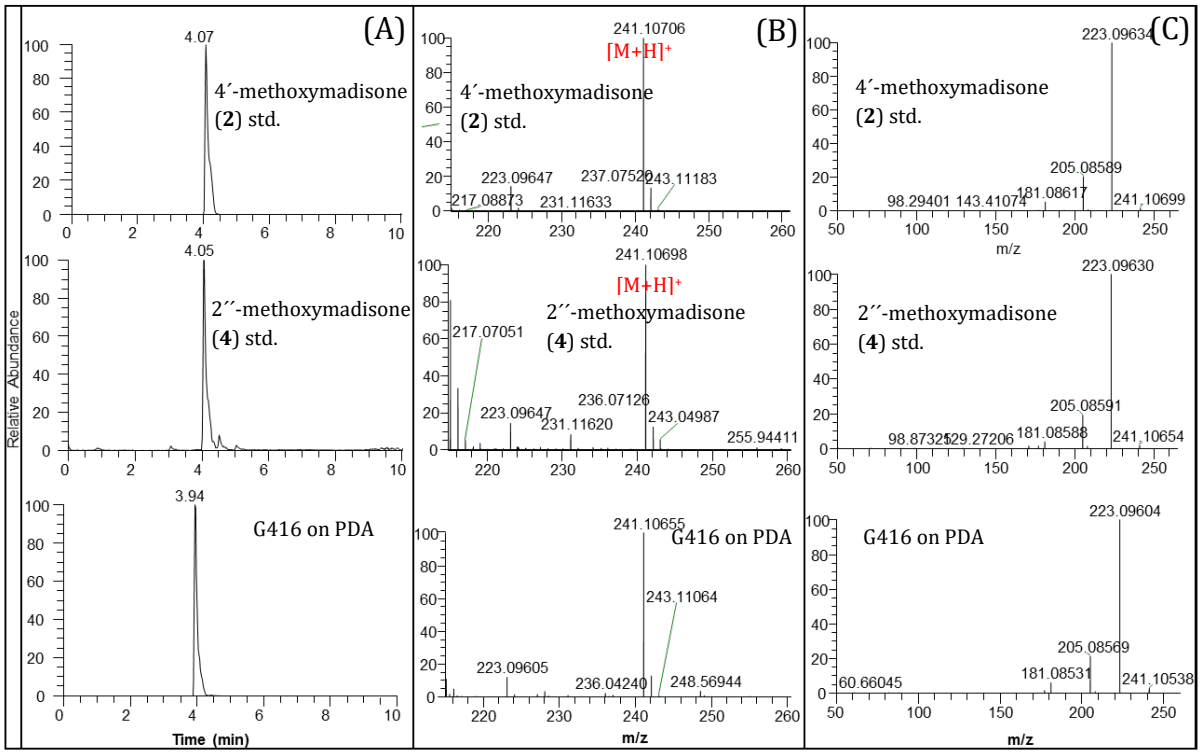

Figure S18. (A) Overlay of chromatographic peaks of **2** and **4** (B) (+)-HRESIMS of **2** and **4** (C) MS/MS HCD fragmentation of **2** and **4**. The top and bottom show the data for the reference standard and *in situ* analysis of G416 grown on PDA, respectively.

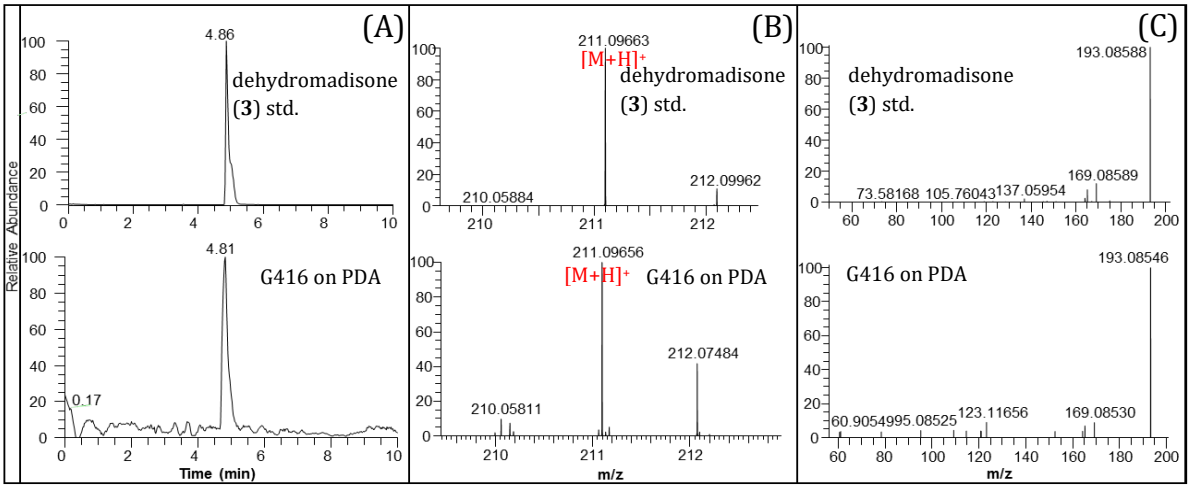

Figure S19. (A) Overlay of chromatographic peaks of **3** (B) (+)-HRESIMS of **3** (C) MS/MS HCD fragmentation of **3.** The top and bottom show the data for the reference standard and *in situ* analysis of G416 grown on PDA, respectively.

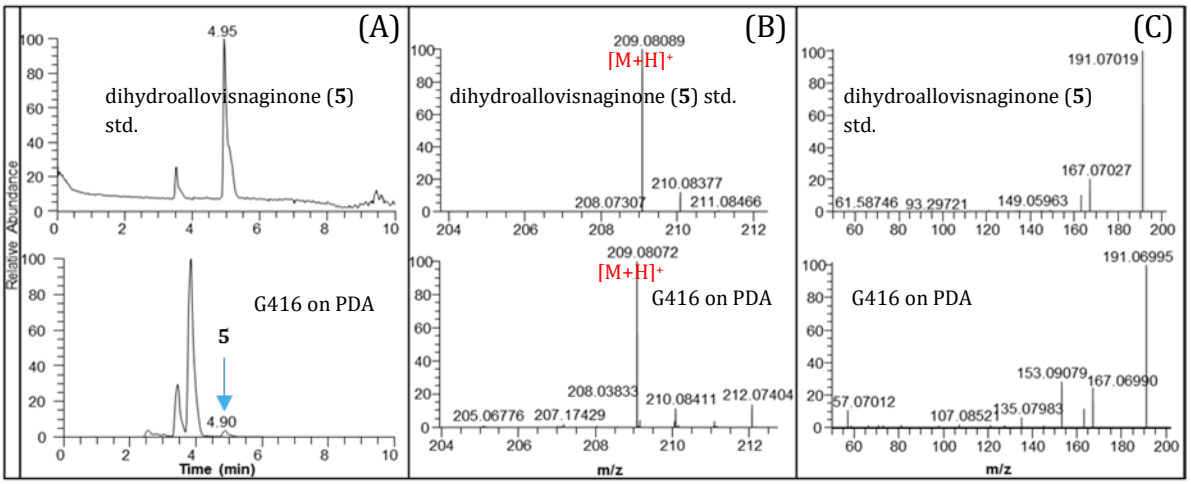

Figure S20. (A) Overlay of chromatographic peaks of **5** (B) (+)-HRESIMS of **5** (C) MS/MS HCD fragmentation of **5.** The top and bottom show the data for the reference standard and *in situ* analysis of G416 grown on PDA, respectively.

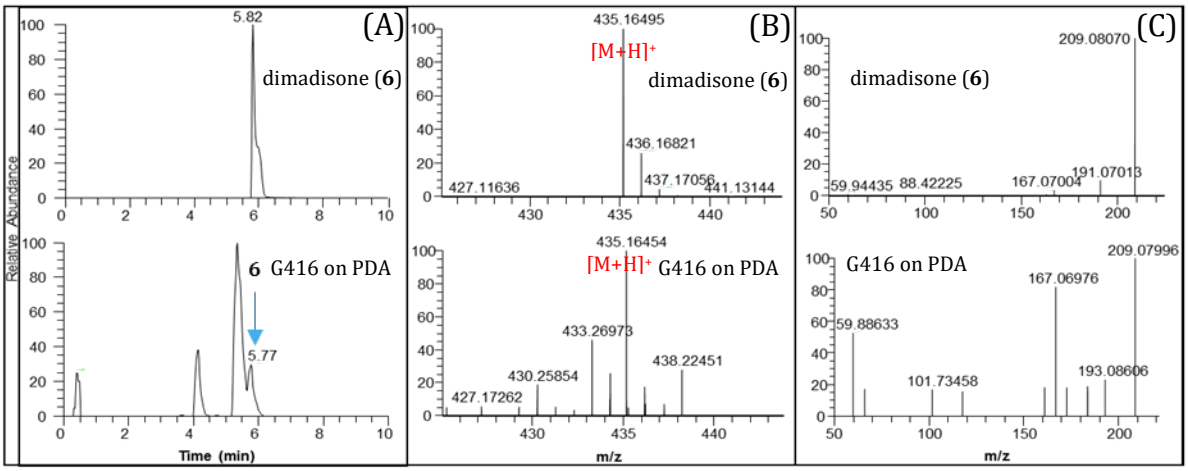

Figure S21. (A) Overlay of chromatographic peaks of **6** (B) (+)-HRESIMS of **6** (C) MS/MS HCD fragmentation of **6.** The top and bottom show the data for the reference standard and *in situ* analysis of G416 grown on PDA, respectively.

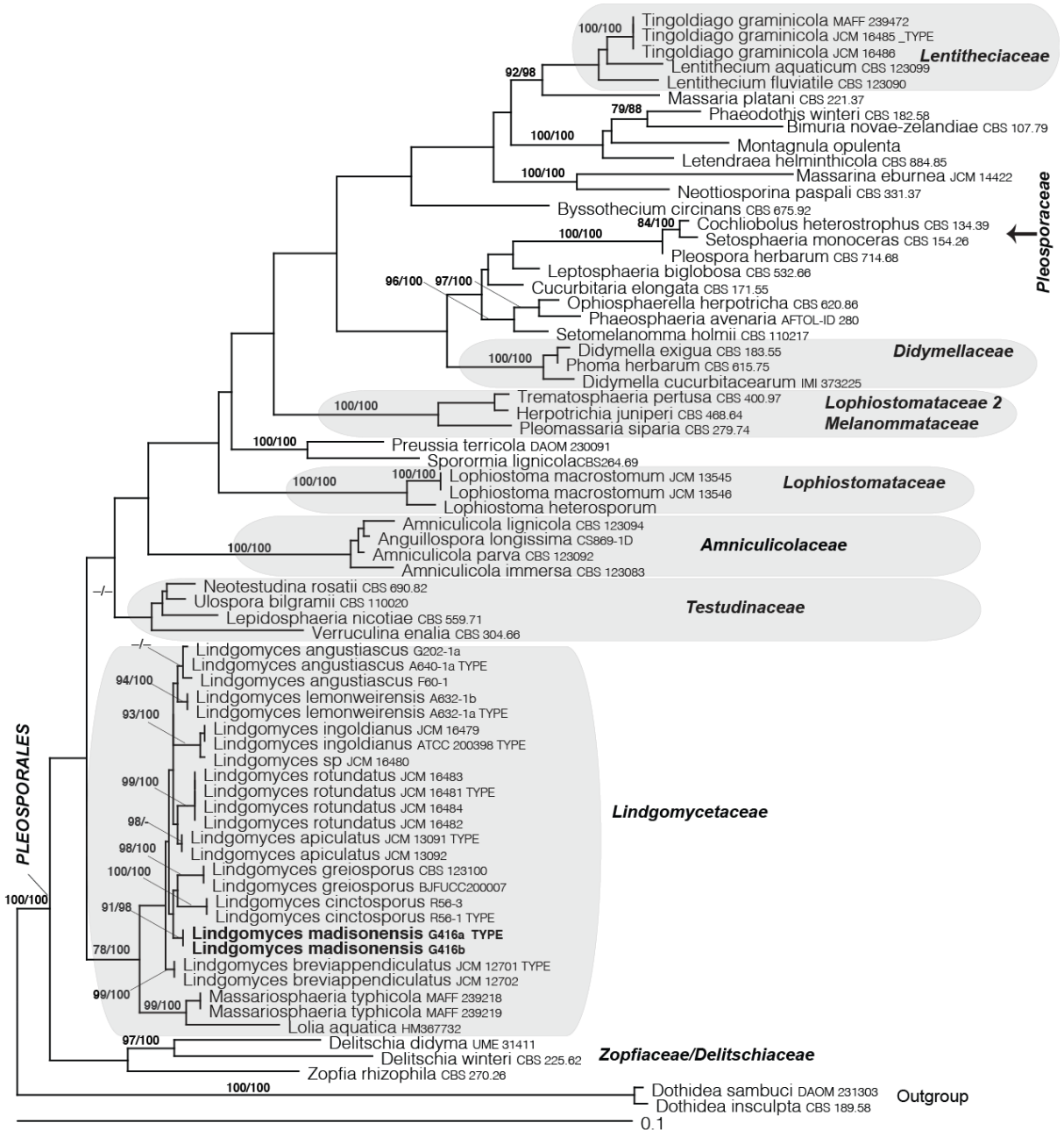

Figure S22. Phylogram of the most likely tree (-lnL = 10047.29) from a RAxML analysis of 70 taxa based on combined SSU and LSU nrDNA sequence data (2309 bp). Numbers refer to RAxML bootstrap support values ≥ 70 % based on 1000 replicates and significant Bayesian posterior probabilities ≥ 95 %. New species of strain G416 is indicated in bold and is identified as having phylogenetic affinities to members of the freshwater ascomycete genus *Lindgomyces.* Bar indicates nucleotide substitutions per site.

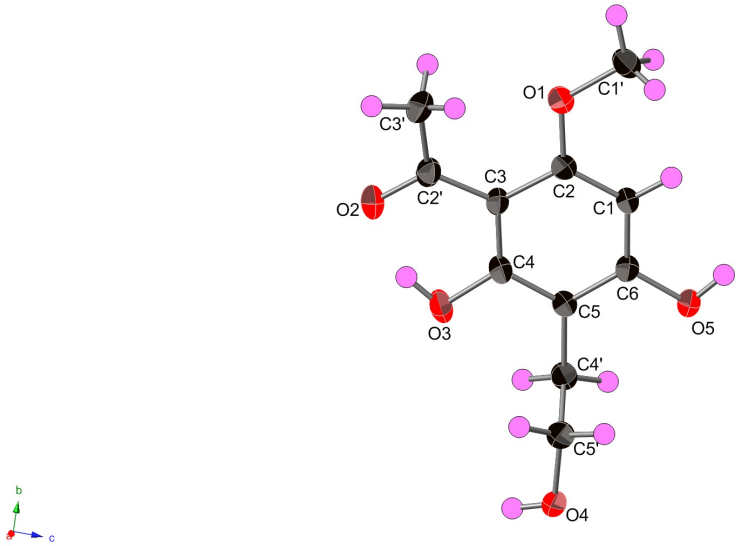

Figure S23. The molecular structure of **1** depicted with 50% probability displacement ellipsoids.

Table S1. Crystal data, data collection, and refinement details.

Crystal data

$C_{11}H_{14}O_5$	D_x = 1.393 Mg m^{-3}
M_r = 226.22	Mo $K\alpha$ radiation, λ = 0.71073 Å
Orthorhombic, $P2_12_12_1$	Cell parameters from 4245 reflections
a = 4.3710 (4) Å	θ = 3.5–28.2°
b = 11.6045 (11) Å	μ = 0.11 mm^{-1}
c = 21.2672 (19) Å	T = 193 K
V = 1078.74 (17) Å^3	Irregular, colourless
Z = 4	0.29 × 0.16 × 0.03 mm
F(000) = 480	

Data collection

Bruker APEX CCD diffractometer	3150 independent reflections
Radiation source: sealed tube	2720 reflections with $I > 2\sigma(I)$
Graphite monochromator	R_{int} = 0.040
ϕ and ω scans	θ_{max} = 30.0°, θ_{min} = 3.5°
Absorption correction: multi-scan data were corrected for scaling and absorption effects using the multi-scan technique (*SADABS*). The ratio of minimum to maximum apparent transmission was 0.986. The calculated minimum and maximum transmission coefficients (based on crystal size) are 0.969 and 0.997.	h = -6→6
T_{min} = 0.735, T_{max} = 0.986	k = -16→16
15607 measured reflections	l = -29→29

Refinement

Refinement on F^2	Primary atom site location: structure-invariant direct methods
Least-squares matrix: full	Secondary atom site location: difference Fourier map
$R[F^2 > 2\ \sigma(F^2)] = 0.042$	Hydrogen site location: mixed
$wR(F^2) = 0.109$	H atoms treated by a mixture of independent and constrained refinement
$S = 1.03$	$w = 1/[\sigma^2(F_o^2) + (0.0583P)^2 + 0.116P]$ where $P = (F_o^2 + 2F_c^2)/3$
3150 reflections	$(\Delta/\ \sigma)_{max} = 0.001$
159 parameters	$\Delta\rangle_{max} = 0.32$ e Å^{-3}
0 restraints	$\Delta\rangle_{min} = -0.14$ e Å^{-3}

Special details

Geometry. All esds (except the esd in the dihedral angle between two l.s. planes) are estimated using the full covariance matrix. The cell esds are taken into account individually in the estimation of esds in distances, angles and torsion angles; correlations between esds in cell parameters are only used when they are defined by crystal symmetry. An approximate (isotropic) treatment of cell esds is used for estimating esds involving l.s. planes.

Table S2. Antimicrobial activities of compounds **1**, **2**, and **5**.

Compound	Minimum inhibitory concentration (µg/mL)				
	S. aureus	*E. coli*	*M. smegmatis*	*C. albicans*	*A. niger*
1	>55	>55	>55	>55	>55
2	>55	>55	>55	>55	>55
5	>55	>55	>55	>55	>55